THE FINER THINGS IN LIFE: COMPARING HIGH RESOLUTION FOSSIL FUEL CARBON DIOXIDE EMISSIONS INVENTORIES

A Thesis
by
MAYA GABRIELLE HUTCHINS

Submitted to the Graduate School
at Appalachian State University
in partial fulfillment of the requirements for the degree of
MASTER OF ARTS

August 2014
Department of Geography

THE FINER THINGS IN LIFE: COMPARING HIGH RESOLUTION FOSSIL FUEL CARBON DIOXIDE EMISSIONS INVENTORIES

A Thesis
by
MAYA GABRIELLE HUTCHINS
August 2014

APPROVED BY:

_____
Jeffrey D. Colby
Chairperson, Thesis Committee

_____
Gregg Marland
Co-Chairperson, Thesis Committee

_____
Eric Marland
Member, Thesis Committee

_____
Kathleen Schroeder
Chairperson, Department of Geography and Planning

_____
Max C. Poole, Ph.D.
Dean, Cratis Williams Graduate School

Abstract

THE FINER THINGS IN LIFE: COMPARING HIGH RESOLUTION FOSSIL FUEL CARBON DIOXIDE EMISSIONS INVENTORIES

Maya Gabrielle Hutchins
B.S., Appalachian State University
M.A., Appalachian State University

Chairperson: Jeffrey D. Colby
Co-Chairperson: Gregg Marland

The quantification of fossil fuel contributions to carbon dioxide concentrations is necessary in order to accurately represent carbon cycle fluxes and to support climate change research. In addition, the monitoring, reporting, and verification of carbon dioxide emissions is necessary for the success of international agreements to reduce emissions. However, existing fossil fuel carbon dioxide ($FFCO_2$) emissions inventories vary in terms of the data and methods used to estimate and distribute $FFCO_2$. This paper will compare how the approaches used to create $FFCO_2$ emissions inventories effect the magnitude and spatial distribution of emissions estimates. Five $FFCO_2$ emission inventories were compared: Carbon Dioxide Information and Analysis Center (CDIAC), Emission Database for Global Atmospheric Research (EDGAR), Fossil Fuel Data Assimilation System (FFDAS), Open-source Data Inventory for Anthropogenic CO_2 (ODIAC), and Vulcan. The effects of using specific data and approaches in the creation of spatially explicit $FFCO_2$ emissions inventories, and the effect of resolution on data representation are analyzed using graphical, numerical, and cartographic data. Data were compared using spatial correlation, the sum of

absolute differences, logarithmic plots, cumulative emissions curves, distribution curves, and spatial distribution maps to understand the effects of using top-down versus bottom-up approaches, nightlights versus population, and the inclusion of large point sources. The results indicate that the approach used to distribute emissions in space creates distinct patterns in the magnitudes and distribution of emissions estimates. Understanding the relationship between these patterns and how they change with resolution supports future development of gridded $FFCO_2$ emissions inventories.

Acknowledgments

I would like to thank my committee members, Dr. Gregg Marland, Dr. Jeffrey Colby, Dr. Eric Marland, and Dr. Kathleen Schroeder for their invaluable support and for the enthusiasm and passion that they have instilled in me. They are all amazing mentors and role models for the kind of researcher and scientist I aspire to be.

I would like to thank Dr. Tom Oda, Dr. Kevin Gurney, and Dr. Bob Andres for all of the help and patience they have showed me as I began my journey in this field of study. Without their support and time this research would not have been possible.

The Carbon Monitoring System Program (NNH11ZDA001N-CMS) of the U.S. National Aeronautics and Space Administration supported this research.

Dedication

I dedicate this thesis to my grandma Nancy, my grandma Amy, and to my parents Connie and Bill. Without all of their loving support I would not have made it to where I am today.

Table of Contents

List of Tables

List of Figures

Foreword

The main body of this thesis will be submitted to *Global Biogeochemical Cycles*, an international journal publishing peer-reviewed articles; it has been formatted according to the style guide for that journal. The journal is published by the American Geophysical Union (AGU).

1.1.Introduction

Anthropogenic sources of carbon dioxide emissions result from the manufacture of cement, the destruction of forests, and the consumption of coal, petroleum, and natural gas. In 2011, the global atmospheric concentration of CO_2 had increased by 40% since 1750, primarily from fossil fuel emissions [*Hartmann et al.*, 2013]. Fossil Fuel Carbon Dioxide ($FFCO_2$) emissions inventories describe CO_2 emissions from fossil fuel combustion at different scales and resolutions.

In general, the scale at which human and physical systems are modeled and represented are important because physical processes cannot be successfully modeled unless data are available at an appropriate scale and at the defined level of detail [*Goodchild*, 2001]. How the world is described determines the kind of science that can be done with the description, making the level of detail of geographic data one of its most important properties [*Goodchild,* 2001]. The four meanings of scale, as defined by *Cao and Lam* [1997], are 1) cartographic or map scale, 2) geographic or observational scale, 3) operational scale and 4) measurement of scale [*Cao and Lam,* 1997]. The two types of scale related to digital geographic data are measurement scale, scale as the level of detail of description, and geographic scale, scale as the extent of area covered [*Cao and Lam,* 1997; *Goodchild*, 2001, 2011].

This paper investigates how the difference approaches used in the creation of ($FFCO_2$) emissions inventories effect the magnitude and spatial distribution of emissions estimates at sub-national scales. In addition, the effect of scale and resolution on the representation

of $FFCO_2$ emissions was examined. This paper will use the two meanings of scale most related to digital data: geographic scale (extent) and measurement scale (resolution) [*Cao and Lam*, 1997; *Goodchild*, 2001, 2011]. Specifically, the magnitude and spatial distribution of five spatially explicit $FFCO_2$ data sets were compared for the Continental United States at a range of scales using a geographic information system (GIS). The datasets analyzed include the Carbon Dioxide Information and Analysis Center (CDIAC), the Emission Database for Global Atmospheric Research (EDGAR), the Fossil Fuel Data Assimilation System (FFDAS), the Open-source Data Inventory for Anthropogenic CO_2 (ODIAC), and Vulcan (Table 1). $FFCO_2$ emissions inventories were analyzed for the years 2002 and 2008 due to the limited temporal scale of Vulcan, available only for the year 2002, and ODIAC, available only for the year 2008.

Detailed methods for estimating the spatial distribution of fossil fuel carbon dioxide emissions vary and no comprehensive comparison of datasets has previously been performed. Such comparisons are necessary to understand the importance of using different data and approaches in the creation of spatially explicit $FFCO_2$ emissions inventories. Additionally, issues of scale and resolution are traditionally important issues in geography, and as GIS's have advanced, multi-scale data is starting to play a more important role in studies such as global change [*Cao and Lam*, 1997]. Both geographic scale and measurement scale have large implications for the development and use of $FFCO_2$ emissions inventories.

This analysis will evaluate the difference between more time consuming methods like those used in bottom-up inventories and less detailed top-down approaches. Comparisons of the different approaches will inform future development of gridded distributions of FFCO2 emissions and their associated uncertainty with the ultimate goal of creating a detailed yet globally consistent FFCO2 emissions inventory. A variety of graphical and numerical methods were employed to compare the existing, spatially-explicit FFCO2 data sets and to explore how their methods and selection of proxy data are reflected in their final products. Comparisons between datasets were conducted using metrics found in similar analyses of FFCO2 datasets [e.g., *Andres et al.*, 1996; *Marland et al.*, 1999; *Gregg and Andres*, 2008; *Gurney et al.*, 2009; *Rayner et al.*, 2010; *Andres et al.*, 2011; *Oda and Maksyutov*, 2011] including spatial correlation, sum of absolute differences, and difference maps. Cumulative emissions curves, distribution curves, and spatial distribution maps were also analyzed to lend greater insight into the relationships between emissions inventories. The data sets were compared at various levels of aggregation to assess how the virtues of each emissions inventory can best be utilized.

1.2. The Author's Role in the Article Section of this Research

The primary author for the manuscript submitted as a part of this thesis to meet the Cratis D. Williams Graduate School requirement for completion of the Master of Arts in Geography acquired the data from its sources, imported and converted the data to usable formats, and analyzed the data. With guidance from her thesis committee she drafted the manuscript that will be submitted to Global Biogeochemical cycles, an international journal associated with the American Geophysical Union that publishes peer-reviewed research.

A Comparison of Five High-resolution Spatially-explicit Fossil Fuel Carbon Dioxide Emissions Inventories

Maya G. Hutchins and Jeffrey D. Colby, Department of Geography and Planning, Appalachian State University, Boone, North Carolina, USA.

Gregg Marland, Research Institute for Environment, Energy, and Economics, Appalachian State University, Boone, North Carolina, USA.

Eric Marland, Department of Mathematical Sciences, Appalachian State University, Boone, North Carolina, USA.

Corresponding author: Maya G. Hutchins, Department of Geography and Planning, Appalachian State University, Boone, NC, USA (hutchinsmg@appstate.edu)

Key Points

- Approaches used for spatially distributing $FFCO_2$ emissions estimates matter
- Spatial uncertainty across $FFCO_2$ emissions inventories needs to be addressed
- Issues of scale and resolution related to FFCO2 emissions inventories need to be addressed
- More detailed metadata are needed to fully utilize $FFCO_2$ emissions inventories

Abstract

The quantification of fossil fuel contributions to carbon dioxide concentrations is necessary in order to accurately represent carbon cycle fluxes and to support climate change research. In addition, the monitoring, reporting, and verification of carbon dioxide emissions is necessary for the success of international agreements to reduce emissions. However, existing fossil fuel carbon dioxide ($FFCO_2$) emissions inventories vary in terms of the data and methods used to estimate and distribute $FFCO_2$. This paper will compare how the approaches used to create $FFCO_2$ emissions inventories effect the magnitude and spatial distribution of emissions estimates. Five $FFCO_2$ emission inventories were compared: Carbon Dioxide Information and Analysis Center (CDIAC), Emission Database for Global Atmospheric Research (EDGAR), Fossil Fuel Data Assimilation System (FFDAS), Open-source Data Inventory for Anthropogenic CO_2 (ODIAC), and Vulcan. The effects of using specific data and approaches in the creation of spatially explicit $FFCO_2$ emissions inventories, and the effect of resolution on data representation are analyzed using graphical, numerical, and cartographic data. Data were compared using spatial correlation, the sum of absolute differences, logarithmic plots, cumulative emissions curves, distribution curves, and spatial distribution maps to understand the effects of using top-down versus bottom-up approaches, nightlights versus population, and the inclusion of large point sources. The results indicate that the approach used to distribute emissions in space creates distinct patterns in the magnitudes and distribution of emissions estimates. Understanding the relationship between these patterns and how they change with resolution supports future development of gridded $FFCO_2$ emissions inventories.

Index Terms and Keywords

1928 GIS science

0434 Data sets

0478 Pollution: urban, regional, and global

Fossil Fuel Emissions

Carbon Dioxide

Emission Inventories

Anthropogenic Emissions

1. Introduction

Anthropogenic sources of carbon dioxide emissions result from the manufacture of cement, the destruction of forests, and the consumption of coal, petroleum, and natural gas. In 2011, the global atmospheric concentration of CO_2 had increased by 40% since 1750, primarily from fossil fuel emissions [*Hartmann et al.*, 2013]. Fossil Fuel Carbon Dioxide ($FFCO_2$) emissions inventories describe CO_2 emissions from fossil fuel combustion at different scales and resolutions.

This paper investigates how the difference approaches used in the creation of ($FFCO_2$) emissions inventories effect the magnitude and spatial distribution of emissions estimates at sub-national scales. In addition, the effect of scale and resolution on the representation of $FFCO_2$ emissions was examined. This paper will use the two meanings of scale most related to digital data: geographic scale (extent) and measurement scale (resolution) [*Cao and Lam*, 1997; *Goodchild*, 2001, 2011]. Specifically, the magnitude and spatial distribution of five spatially explicit $FFCO_2$ data sets were compared for the Continental United States at a range of scales using a geographic information system (GIS). The datasets analyzed include the Carbon Dioxide Information and Analysis Center (CDIAC), the Emission Database for Global Atmospheric Research (EDGAR), the Fossil Fuel Data Assimilation System (FFDAS), the Open-source Data Inventory for Anthropogenic CO_2 (ODIAC), and Vulcan (Table 1). $FFCO_2$ emissions inventories were analyzed for the years 2002 and 2008 due to the limited temporal scale of Vulcan, available only for the year 2002, and ODIAC, available only for the year 2008.

Detailed methods for estimating the spatial distribution of fossil fuel carbon dioxide emissions vary and no comprehensive comparison of datasets has previously been performed. Such comparisons are necessary to understand the importance of using different data and approaches in the creation of spatially explicit $FFCO_2$ emissions inventories. Additionally, issues of scale and resolution are traditionally important issues in geography, and as GIS's have advanced, multi-scale data is starting to play a more important role in studies such as global change [*Cao and Lam,* 1997]. Both geographic scale and measurement scale have large implications for the development and use of $FFCO_2$ emissions inventories.

This analysis will evaluate the difference between more time consuming methods like those used in bottom-up inventories and less detailed top-down approaches. Comparisons of the different approaches will inform future development of gridded distributions of FFCO2 emissions and their associated uncertainty with the ultimate goal of creating a detailed yet globally consistent FFCO2 emissions inventory. A variety of graphical and numerical methods were employed to compare the existing, spatially-explicit FFCO2 data sets and to explore how their methods and selection of proxy data are reflected in their final products. Comparisons between datasets were conducted using metrics found in similar analyses of FFCO2 datasets [e.g., *Andres et al.*, 1996; *Marland et al.*, 1999; *Gregg and Andres*, 2008; *Gurney et al.*, 2009; *Rayner et al.*, 2010; *Andres et al.*, 2011; *Oda and Maksyutov*, 2011] including spatial correlation, sum of absolute differences, and difference maps. Cumulative emissions curves, distribution curves, and spatial distribution maps were also analyzed to lend greater insight into the relationships

between emissions inventories. The data sets were compared at various levels of aggregation (0.1°, 0.5°, 1°, 2°, and 3°) to assess how the virtues of each emissions inventory can best be utilized.

1.1.1. A Brief Overview

Fossil fuel carbon dioxide ($FFCO_2$) emissions are historically estimated at national and annual scales from national level energy statistics published by either the International Energy Agency (IEA), the United Nations (UN), British Petroleum Corporation (BP), the U.S. Department of Energy/Energy Information Administration (DOE/EIA), or the U.S. Environmental Protection Agency (EPA) (see table 1). Energy statistics are often divided into sectors and/or fuel types, and emissions per fuel type are calculated from emissions factors, the ratio of pollutant emitted per unit of fossil fuel burned. There are now five widely used emissions inventories that use one or more of the national level energy statistics published by the above agencies to estimate CO_2 emissions at the national level: IEA, CDIAC, USDOE/EIA, BP, and EDGAR (see Table 1). All of these emissions inventories are global or national, and annual in scale. However, the "emphases, categories, units, unit conversions and reporting, data processing, and quality assurance" of energy statistics vary across organizations, leading to variability in the estimated magnitudes of emissions [*Andres et al.*, 2012].

1.1.2. Fine Resolution Emissions Inventories

Despite increasing concern for the impacts of increasing concentrations of carbon dioxide in the atmosphere, little work has been done to estimate the seasonal flux or the sub-

national distribution of carbon dioxide emissions [*Gregg and Andres,* 2008] As a result, modern climate change research is struggling to make accurate projections of future climatic changes and informative assessments of biogeochemical feedbacks within the carbon cycle [*Gurney et al.,* 2009; *Oda and Maksyutov,* 2011; *Andres et al.,* 2011]. Fossil fuel consumption statistics were historically compiled at national extents because energy data were generally available at large scales, and questions regarding global climate change during the twentieth century did not require data at smaller scales. Recent climate and carbon science, as well as public policy, necessitates an increase in the spatio-temporal resolution of fossil fuel carbon dioxide emissions inventories [*Gurney et al.,* 2009; *Andres et al.,* 2011].

Finer resolution $FFCO_2$ emissions inventories seek to estimate the location of $FFCO_2$ emissions at the subnational scale (extent) and resolutions of 1° or finer. Fossil fuel carbon dioxide estimates are used as *a priori* information in carbon flux models to distinguish between human and natural sources of carbon dioxide and supporting evidence for anthropogenic contributions to carbon dioxide emissions relies on "bottom-up" inventories of $FFCO_2$ emissions [*Rayner et al.,* 2010; *Andres et al.,* 2011]. More specifically, spatially distributed $FFCO_2$ emissions are necessary to identify areas of pollution concentration for inputs into air simulation models and result in decreased errors in dispersion emissions transport models [*Dai and Rocke,* 1999; *Wang et al.,* 2012]. Carbon flux models require the input of carbon dioxide sources and sinks, which depend on $FFCO_2$ inventories to distinguish between natural and anthropogenic sources of CO_2. Furthermore, spatially explicit $FFCO_2$ emissions inventories lend insight into the

relationship between fossil fuel use and economic strength, [*Andres et al.*, 2011]. By improving the spatial and temporal resolution of bottom-up emissions inventories it may be possible to corroborate atmospheric composition with remotely sensed data, making confirmation of international emissions estimates possible [*Andres et al.*, 2011]. The magnitude and spatial distribution of $FFCO_2$ emissions at fine resolutions are necessary for monitoring, reporting, and verifying carbon emissions, and will become increasingly important as cap and trade programs or other emissions mitigation programs are developed and the global community continues to move toward a global emissions agreement.

In response to the need for sub-national data on $FFCO_2$ emissions, there has been increasing interest in creating spatially explicit $FFCO_2$ emissions inventories at resolutions of 1° or finer. Finer resolution emissions inventories are created using three primary methodologies (top-down approaches, bottom-up approaches, and data assimilation) and two primary data types (non-point source and point-source information). However, non-point source data is not distinct from point-source data. In this analysis we make a distinction between emissions from small point sources and large point sources (LPS). Small point sources of emissions, such as homes and small businesses, are statistically treated as areal (non-point) sources in emissions inventories. Large point sources describe emissions from large facilities related to the generation of electric power, industrial processes, and petroleum refineries. However, data are not generally available to characterize emissions from industrial facilities and refineries at the

global scale. The term LPS in this paper refers strictly to emissions from large electric power generating facilities.

Non-point source $FFCO_2$ emissions estimates are derived from the national level CO_2 emissions inventories referenced previously (IEA, CDIAC, USDOE, BP, and EDGAR). Non-point source data is disaggregated from the national scale to subnational scales and finer resolutions using top-down approaches. Top down approaches generally utilize proxies such as population and/or satellite-observed nightlights data to distribute emissions in space [*Andres et al.,* 1996; *Gurney et al.,* 2009; *Rayner et al.,* 2010; *Andres et al.,* 2011; *Oda and Maksyutov,* 2011; *Wang et al.,* 2012]. The resolution of spatially explicit $FFCO_2$ emissions inventories that utilize a top-down approach rely on the resolution of the proxy data being used for the disaggregation of emissions in space. Data assimilation uses observational data to constrain dynamic models, such as the Kaya identity, which estimates CO_2 emissions using data on population, gross domestic production (GDP), and energy consumption [*Rayner* et al., 2010]. Bottom-up approaches generally involve data collection on fuel consumption or emissions at the building scale or lower and sum individual sources of emissions to estimate $FFCO_2$ emissions at the county-, state-, or national scales [*Gurney et al.,* 2009].

Emissions from large point sources account for approximately 40% of total national emissions in most countries [*Singer et al.,* 2014]. As a result, emissions from LPS have been recently utilized in the development of spatially explicit $FFCO_2$ emissions inventories and have been incorporated into top-down, bottom-up, and data assimilation

approaches. Emissions from LPS of $FFCO_2$ are estimated using material balance calculations and continuous emissions monitors (CEMs). Material balance approaches multiply the difference between the amount of material entering a process and the final product by an emissions factor to estimate the CO_2 emissions that result from a specific process. LPS emissions data are available from the U.S. EPA, the U.S. DOE/EIA, and the Center for Global Development. The U.S. EPA publishes three data sets on LPS emissions, the Emissions & Generation Resource Integrated Database (eGRID), the National Emissions Inventory (NEI), and the Greenhouse Gas Reporting Program (GHGRP). The GHGRP and NEI include emissions estimates from all LPSs, while eGRID estimates CO_2 emissions from electrical generation only. The NEI reports emissions of carbon monoxide (CO) from point sources in the U.S., which can be converted to estimate CO_2 emissions using emissions factors. The Center for Global Development publishes CARMA (Carbon Monitoring for Action), which reports emissions of CO_2 from electric power plants globally.

2. Data and Methods

2.1.Data

Materials used in this analysis include five data sets on $FFCO_2$ emissions inventories for the U.S. A comparison is made among the five $FFCO_2$ emissions inventories for similarities and differences in the energy statistics used, the sectors included, and most significantly, the methods used for spatial disaggregation or allocation of emissions (Table 1).

FFDAS was created using a data-assimilation approach and uses energy statistics from the International Energy Agency (IEA). Observational data from population and nightlight data are used to constrain a predictive model known as the Kaya identity, which estimates the flux of $FFCO_2$ emissions through a region. Sectors in FFDAS are based on IEA emissions sectors, including emissions from commercial electricity generation, manufacture, international and domestic transport, and emissions from other sectors such as residential, agriculture, and fishing. It is important to note that FFDAS does not include emissions from industrial processes such as calcining limestone in the manufacture of cement [*Rayner et al.*, 2010]. While data assimilation is a slightly different approach for estimating the location of $FFCO_2$ than top-down approaches, for the analysis performed in this paper top-down will be used to refer to both traditional top-down approaches and data assimilation approaches.

The EDGAR data set was created using a top-down approach and utilizes activity data primarily based on energy statistics produced by the IEA, but supplemented by data from the United Nations (U.N.), as well as from commercial firms that compile industry statistics [*Marland et al.*, 1999; *EDGARv4 methodology*, unpublished report, available at *http://edgar.jrc.ec.europa.eu/methodology.php*] EDGAR includes emissions from fuel combustion, fugitive emissions from fuel use, industrial processes such as cement manufacture, non-energy use of lubricants/waxes, and solvent and other product uses. Emissions are calculated for the years 2000 to 2010. Emissions are distributed on a 0.1° grid using the location of energy and manufacturing facilities, road networks, shipping

routes, and population density [*Andres et al.*, 2012; *EDGARv4 methodology*, unpublished report, available at *http://edgar.jrc.ec.europa.eu/methodology.php*].

The CDIAC data set was created using a top- down approach, where nationally aggregated emissions are distributed on a regular 1° grid using a 1984 population distribution data set from the Goddard Institute of Space Studies (GISS). CDIAC relies on energy statistics produced by the United Nations (U.N.) and includes emissions from fossil fuel burning, cement manufacture, and gas flaring in oil fields [*Andres et al.*, 1996; *Marland et al.*, 1999]. CDIAC data spans the longest time period, from 1751 to 2010 [*Andres et al.*, 1996].

The ODIAC data set was created using a top-down approach which disaggregates national emissions estimates produced by CDIAC, but distributes them using nightlight data and the location of LPS inventoried in CARMA. ODIAC is published at the same resolution as the nightlight data, approximately 1 km, or 0.008333°, for the year 2008 [*Oda and Maksyutov*, 2011].

The Vulcan data set was created using a bottom-up approach and utilizes 7 primary datasets to estimate $FFCO_2$ emissions. Vulcan uses CO_2 emissions directly when estimates are available, or CO emissions and CO_2 emissions factors as an alternative when CO_2 emissions are not reported. Vulcan estimates emissions from air transport, commercial, industrial, and residential energy use, cement manufacturing, utilities, and non-road and on-road mobile activities [*Gurney et al.*, 2009]. Emissions from LPSs are

retrieved from the EPA/EIA NEI and the EPA CAMD ETS/CEMs data. County-level road- specific emissions are distributed using a GIS road-atlas with twelve road types falling under the more general road classifications of rural and urban. Non-point source emissions are available from the NEI at the county scale, and are downscaled to census tracts using the total floor square footage of industrial, commercial, and residential buildings within each census tract [*Gurney et al.,* unpublished report, available at http://vulcan.project.asu.edu/pdf/Vulcan.documentation.v2.0.online.pdf]. The data is then rendered to a regular 10 km grid using area-based weighting [*Gurney et al.,* 2009). Vulcan is considered to be the most accurate $FFCO_2$ emissions inventory, but data on $FFCO_2$ emissions at the subnational scale are not very common, and are usually collected for very specific purposes [*Andres et al.,* 2012]. Due to limited data availability at subnational resolutions, bottom- up approaches are currently constrained to regional scales and shorter time scales. Vulcan is thus available only for the year 2002 and is limited to the U.S. in terms of spatial extent.

2.2.Methods

Data files representing the five emissions data sets were acquired from their authors and imported into ArcGIS (ESRI 2014. ArcGIS Desktop: Release 10.1. Redlands, CA: Environmental Systems Research Institute) using geographic coordinate system (GCS) WGS84.

There are two primary referencing systems that assign data to a geographic location on the surface of the earth (geo-referencing system). A spherical coordinate system

represents locations of a feature in latitude and longitude in units of degree, minutes and seconds on a spherical grid. However, rather than dealing with a curved surface, it can be more useful to represent the earth's surface on a flat plane. For example, paper maps are flat, a planar representation is required to see all of Earth at one time, and it is much easier to measure distances on a plane. Because Earth is not a perfect sphere, representing Earth on a planar surface involves representing the Earth as a 'best fit' ellipsoid. Initially, countries adopted their own ellipsoid models. However, because the earth is not shaped like a perfect ellipsoid, each ellipsoid representation of the earth may have better fits to different geographic regions on the globe. Today, an international standard ellipsoid for representing the globe has been adopted, known as the World Geodetic System (WGS84). The decision to use GCS WGS84 for this study is based on discussions with the authors of FFDAS and ODIAC. When no geo-referencing was specified beyond spherical coordinates the data were displayed using a WGS84 ellipsoid model. Total $FFCO_2$ emissions were calculated for each inventory's largest available extent using zonal statistics in ArcGIS and compared to the author-documented totals to ensure the data were read correctly into the GIS.

All data were analyzed for the continental U.S. only, where the U.S. is defined as all grid spaces in Vulcan with non-zero values. After the global data sets were masked to the extent of the Vulcan inventory, national level emissions were calculated using zonal statistics in ArcGIS. Since the data are masked to the extent of the Vulcan inventory, comparisons between emissions inventories occur only at locations where Vulcan has non-zero values. At the 0.1° resolution the maximum number of cells included in the

comparison is 81,841 grid cells. There are 928 grid cells at 1° resolution. The scale of this analysis is limited to the continental U.S. because Vulcan, which is considered the most detailed data set, is limited to the United States. Vulcan is also limited to the year 2002 so comparisons are completed for 2002. ODIAC, a fine resolution data set at 1km resolution, is available only for the year 2008, so comparisons are also performed for the year 2008. All other datasets are available for both 2002 and 2008 comparisons.

The data being analyzed were initially acquired at resolutions ranging from 1 km to 1°. In order to make comparisons between emissions inventories at a variety of resolutions, all data were resampled to the same resolution after they were masked to the Vulcan extent. ODIAC was acquired at a 1 km, or 0.008333° resolution, and was aggregated to 0.1° resolution using the aggregation tool in ArcGIS with an aggregation factor of 12 and an aggregation method of sum. Vulcan was analyzed using a 0.1° resolution version of Vulcan produced by the original authors of the data set. It should be noted that the 0.1° data set is provided to assist users with re-gridding and that users are encouraged to re-grid the 10 km resolution data set on their own. The authors of Vulcan assume no responsibility for re-gridding choices that do not match expectation. However, due to the distortions that are inherent with un-projecting geographic data from planar coordinates to spherical coordinates we chose not to re-grid the 10 km Vulcan data set, but to use the 0.1° data set provided by the authors of Vulcan. EDGAR, FFDAS, and Vulcan were acquired at 0.1° resolution. EDGAR, FFDAS, ODIAC, and Vulcan were aggregated from 0.1° resolution to 0.5°, 1°, 2°, and 3° resolutions using the aggregate tool in ArcGIS with an aggregation method of sum and aggregation factors of 5, 10, 20, and 30, respectively.

All data were aggregated from their 0.1° resolution to each of the respective resolutions. CDIAC was acquired at 1° resolution and was aggregated to 2° and 3° resolutions using the aggregate tool in ArcGIS with an aggregation method of sum and aggregation factors of 2 and 3, respectively. The sum aggregation method was used for this analysis because it was necessary to preserve the national total of $FFCO_2$ emissions for each data set across different resolutions. All of the data sets except CDIAC were originally represented at 0.1° resolution or finer, so analyses were conducted at 0.1° and aggregates thereof, except comparisons that included CDIAC at aggregates of 1° and greater.

Comparisons between datasets were conducted using metrics found in similar analyses of $FFCO_2$ datasets [e.g., *Andres et al.,* 1996; *Marland et al.,* 1999; *Gregg and Andres,* 2008; *Gurney et al.,* 2009; *Rayner et al.,* 2010; *Andres et al.,* 2011; *Oda and Maksyutov,* 2011; *Wang et al.,* 2012]. The cumulative emissions curves of each emissions inventory were plotted and compared against each other at 0.1° and 1° resolutions. Emissions were arranged in ascending order and plotted on a logarithmic scale to represent the distribution of emissions magnitudes within the continental U.S. For visual comparison, maps of each data set were generated in ArcGIS at 0.1°, 0.5°, 1°, and 2° resolutions. Difference maps for the most and least correlated pairs of inventories at each resolution (0.1°, 0.5°, 1°, and 2°) were also generated and analyzed.

Spatial correlation coefficients compare the magnitude of one dataset at one location to the magnitude of another data set at the same location, allowing for a numeric comparison of the similarities and differences in the spatial distribution of emissions

inventories. Additionally, the sum of absolute differences is a useful metric for understanding differences in the magnitude of emissions across datasets. The sum of absolute differences and spatial correlation coefficients were calculated between $FFCO_2$ emissions inventories of the same year and resolution. Spatial correlation coefficients were calculated for each data set in MATLAB. $FFCO_2$ emissions inventories were exported from ArcGIS in geotiff format for all resolutions (0.1°, 0.5°, 1°, 2°, and 3°) and imported into MATLAB as matrices. Matrices were reshaped into vector arrays for each resolution using the reshape command in MATLAB. The MATLAB reshape command reshapes a matrix by taking elements from the original matrix in a column-wise approach and rewriting them to an array of the same number of pixels. The vector array of each data set contains the same number of values as the original matrix, and each matrix is reshaped according to the same column-wise approach, so each row in the new vector array represents the same location as the corresponding row in the vector array it is being compared against. After each geotiff matrix was reshaped into vector arrays, the cov and corrcov functions were used to calculate the correlation between each $FFCO_2$ emissions inventory at resolutions of 0.1°, 0.5°, 1°, 2°, and 3°. The cov command creates a covariance matrix between two vectors, and the corrcov command computes a correlation matrix corresponding to the covariance matrix generated by the cov command. Correlation coefficients were calculated for each data set against the others in pairs for relevant resolutions and years. In previous studies the emissions in each dataset were scaled to the same total so that the spatial correlation coefficient was independent of magnitude [*Rayner et al.,* 2010; *Oda and Maksyutov,* 2011]. However, for this analysis the authors believe that both the spatial location and magnitude of emissions are

important when comparing $FFCO_2$ emissions, and the magnitude of emissions is also reflected in the correlation coefficient. The sum of absolute differences (SAD) totals the absolute difference of emissions at each pixel location across all pixels and is used to measure similarity between two images. The sum of absolute differences was calculated in MATLAB by taking the sum of the absolute differences between each set of values in the vector array.

Due to the large range of values contained within each data set, plots of the natural log of each dataset against the other in pairs (Log A versus Log B) emphasizes both high and low emissions values. The natural log of the ratio of two data sets (Log of (A/B)) plotted against the mean of the two data sets (A+B/2) compares the relative magnitude against the absolute value of the two data sets. Using this metric, values will cluster around zero when they are equal, and will be symmetric about the zero axis when they differ by a similar factor [*Marland et al.,* 1999].

Lastly, the role of LPS emissions was examined by comparing the magnitude of each $FFCO_2$ emissions inventory at the location of the top fifty LPS emitting raster cells. LPSs inventoried in eGRID were converted from points to a raster in ArcGIS, so that each grid cell accounted for emissions from multiple eGRID LPSs. The grid cells were then converted back to points, with each point representing all eGRID sources located in a 0.1° cell. The Extract Value to Point tool in ArcGIS was used to retrieve the emissions value of each $FFCO_2$ emissions inventory at the location of the top fifty cells representing emissions from eGRID.

3. Results and Discussion

3.1.Distribution of Emissions

The calculated and author-documented totals of emissions in the five studied datasets are shown in Table 2. After rounding errors the authors assume the documented totals and calculated totals to be equal. ODIAC and FFDAS have the lowest emissions estimates, while Vulcan has the highest. EDGAR author-documented totals varied by source of documentation and whether totals were calculated across sectors or across countries.

Cumulative emissions at 0.1° (Figure 1) show that FFDAS rises in emissions at the slowest rate, indicating that it attributes the majority of emissions to a small number of high emitting cells. ODIAC follows approximately the same cumulative curve as FFDAS, but rises at a slightly faster rate than FFDAS, indicating that ODIAC also assigns more emissions to a small number of high emitting cells compared to the other datasets. ODIAC has nearly half the number of non-zero grid spaces as the other $FFCO_2$ emissions inventories (Figure 2). The 0.1° spatial distribution maps of FFDAS and ODIAC (Figures 3b and 3c) also illustrate this distribution of values, where cells located in less populated areas out west do not contain nightlights and are not assigned emissions values. However, because FFDAS also uses population as a spatial proxy, it attributes emissions to more cells than ODIAC does based on nightlights alone. In both FFDAS and ODIAC emissions are concentrated in urban areas where nightlight values and population density are high. Distribution plots for FFDAS at 0.1° resolution show discrete clustering of emissions values at lower magnitudes (Figure 2). At the 0.1° resolution FFDAS and

ODIAC attribute emissions to cells of the same value at lower magnitudes, creating discrete intervals of emissions. As soon as FFDAS and ODIAC reach lower emissions values, their distribution curves drop to zero (Figure 2).

The cumulative emissions curve for Vulcan at 0.1° rises at a faster rate than both FFDAS and ODIAC, indicating that it attributes more emissions to low and intermediate emitting cells. Vulcan assigns more emissions to the mid-west than either FFDAS or ODIAC. The detailed, fine resolution data used to build the Vulcan $FFCO_2$ emissions inventory allows it to capture emissions in locations that cannot be predicted by nightlights, population, or large point sources alone. Vulcan's detailed methods not only distribute emissions to the west, but also to extensive transportation networks (Figure 3a). Vulcan has the second to largest range of emissions values, just behind EDGAR.

EDGAR's cumulative emissions curve at 0.1° rises at the fastest initial rate, indicating that a larger fraction of EDGAR's emissions are located in low and intermediate cells, and that its emissions values are distributed more evenly, rather than being concentrated in major urban areas. The distribution of emissions at 0.1° (Figure 2) highlights the lower emissions values contained in EDGAR, with the lowest values in EDGAR being orders of magnitude smaller than other $FFCO_2$ emissions inventories. The more uniform distribution of emissions values in EDGAR is shown by the large range of emissions values, with the majority of cells being concentrated between 100 and 10,000 tonnes of C. EDGAR tends to estimate on the low end for major cities and other urban areas, while allocating more emissions to areas surrounding cities (Figure 3d). EDGAR also attributes

a greater amount of emissions out west than FFDAS, ODIAC, or Vulcan. The spatial distribution of EDGAR is unique compared to the other $FFCO_2$ emissions inventories in this analysis, but the documentation for EDGAR is not detailed enough to provide insight into how emissions are distributed and why the data exhibit such unique patterns.

At the 1° resolution CDIAC is also available for comparison and the differences between data sets become less apparent (Figure 4). Similar to 0.1° resolution, EDGAR's cumulative curve at 1° resolution rises at a faster rate than the other emissions inventories, indicating that it attributes more emissions to a greater number of low and intermediate emitting cells. At 1° resolution, CDIAC, FFDAS, ODIAC, and Vulcan follow a similar curve, attributing fewer emissions to low emitting cells. After approximately three-quarters of all grid cells, CDIAC's cumulative emissions curve diverges from FFDAS, ODIAC, and Vulcan, and continues to rise at a slower rate. CDIAC's cumulative emissions rise quickly in the last 100 cells, indicating that CDIAC attributes the majority of its emissions to a lower number of very high emitting cells, and that even less of CDIAC emissions are located in low emitting cells than other emissions inventories. The same distinct intervals of emissions values present in the distribution curve of FFDAS are visible in the distribution curve of CDIAC at 1° resolution (Figure 5). The effect of data aggregation is further shown in the spatial distribution maps at 1° resolution (Figure 6) and 2° resolution (Figure 7). It is important to note that CDIAC assigns values of zero to many cells along the East coast and some along the West coast that Vulcan and the other emissions inventories do not (Figure 6e and Figure 7e).

While the emissions inventories become more similar at 1° resolution, each data set holds distinct patterns of emissions that reflect their respective methods of spatial attribution. In order to further explore the relationships of emissions inventories to each other, correlation coefficients were calculated and plotted on a threshold graph to delineate the relationship between data sets at decreasing resolutions (Figure 8).

Difference maps were calculated for the least and most correlated inventories for the year 2002 at 0.1° and for the years 2002 and 2008 at 1° resolutions. At 0.1° resolution for the year 2002, EDGAR and FFDAS have the lowest correlation, while Vulcan and FFDAS have the highest correlation (Table 3). When FFDAS is subtracted from EDGAR it becomes apparent that EDGAR slightly overestimates in the areas surrounding major urban area, underestimates the majority of the urban area, and then overestimates at the very core of the city with respect to FFDAS (Figure 9a and 9b). A similar pattern appears in the difference map of EDGAR and ODIAC (not shown).

At 1° resolution for the year 2002, CDIAC and FFDAS are the least correlated, while Vulcan and FFDAS are the most correlated (Table 3). At 1° resolution for the year 2008, CDIAC and EDGAR are the least correlated, and ODIAC and FFDAS are the most correlated (Table 4). The difference maps between CDIAC and FFDAS for 2002 (Figure 10a) and CDIAC and EDGAR (Figure 10c) for 2008 are very similar. At 1° resolution, CDIAC tends to overestimate emissions in cells that contain major cities. In some case when CDIAC is compared to FFDAS, CDIAC underestimates for the cell that contains a major city, and overestimates a cell adjacent to it, such as Houston, Cleveland, and

Minneapolis. CDIAC underestimates for Baltimore, Philadelphia, and New York due to zero magnitude cells along the East coast (Figure 10a, 10c, 6e, 7e). The difference maps for the most correlated inventories are similar in that Vulcan and ODIAC both differ the most from FFDAS in urban areas. However, the magnitude difference between FFDAS and Vulcan is much greater than the difference between FFDAS and ODIAC. Vulcan also has more of a tendency to either overestimate or underestimate emissions in major cities compared to FFDAS than ODIAC does when compared to FFDAS.

In an effort to gain more insight into the difference seen between EDGAR and other emissions inventories around urban areas, profiles were taken from the SW to the NE across three major cities, Baltimore, Philadelphia, and New York. Emissions from EDGAR, FFDAS, and ODIAC at the 0.1° resolution were plotted along the transect to further explore the urban distribution of $FFCO_2$ emissions (Figure 11). While all three data sets have good agreement over Baltimore, EDGAR overestimates at the center of both Philadelphia and New York compared to FFDAS and ODIAC. EDGAR similarly overestimates emissions at the core of other major cities, such as Los Angeles, when compared to FFDAS and ODIAC. The tendency for EDGAR to both under estimate and over estimate in comparison to FFDAS, ODIAC, and to a lesser degree, Vulcan, is demonstrated by the 'three-prong' distribution of EDGAR when plotted against FFDAS (Figure 11a), ODIAC (Figure 12b and 12c), and Vulcan (Figure 13a).

Many of the differences and similarities in emissions distributions presented thus far can be related to the methods and data used to create them. In order to make broader

statements about the different approaches used for creating $FFCO_2$ emissions inventories, the relationships between specific datasets are further explored. In addition to analyzing the calculated correlation coefficients, the data are plotted against each other in pairs on a log scale to evaluate differences and similarities in spatial allocation approaches such as top-down versus bottom-up, nightlights versus population, and the treatment of large point sources.

3.1.1. Top down vs. bottom up

While bottom-up emissions inventories such as Vulcan are considered to be more detailed, they are time and labor intensive and encounter both spatial and temporal limitations. Top-down approaches are less detailed but are less costly and are more globally consistent. In order to make comparisons between less intensive top-down approaches and more detailed bottom-up approaches, $FFCO_2$ emissions inventories for the year 2002 were compared against Vulcan. Vulcan is considered to be the most detailed $FFCO_2$ emissions inventory, so $FFCO_2$ emissions inventories that are better correlated with Vulcan may be considered better representations of $FFCO_2$ estimates. The threshold of correlation was graphed for EDGAR, FFDAS, and CDIAC against Vulcan at all comparable resolutions (Figure 8). At 0.1° resolution, the log of FFDAS and EDGAR (2002) were plotted against the log of Vulcan (Figure 13a and 13b). At 1° resolution the log of EDGAR, FFDAS, and CDIAC were plotted against the log of Vulcan (Figure 13c-e).

At the 0.1° resolution, EDGAR and Vulcan have a spatial correlation of 0.43 (Figure 13a, Table 3). FFDAS and Vulcan are the most correlated data sets at 0.1° resolution with a correlation coefficient of 0.62 (Figure 13b, Table 3). However, as indicated by previous results, there is a limitation in FFDAS to discriminate between emissions levels at low emissions magnitudes (13b).

As resolution decreases to 1°, the relationship of EDGAR and FFDAS to Vulcan strengthens with correlation coefficients of 0.94 (Figure 13c) and 0.95 (Figure 9d), respectively (Table 3). At 1° resolution CDIAC is also available for analysis, showing a correlation with Vulcan of 0.39 (Figure 13e, Table 3). As shown in the threshold graph (Figure 8), CDIAC consistently has poor correlation with Vulcan, while FFDAS and EDGAR are best correlated with Vulcan at 1° resolution.

FFDAS underestimates compared to Vulcan (Figure 13c and 13d), which was expected that for this analysis because FFDAS does not contain emissions from cement manufacture while Vulcan does. The exclusion of emissions from cement in FFDAS may significantly lower the correlation between FFDAS and Vulcan. When CDIAC is plotted against Vulcan on a log scale at 1°, CDIAC displays discrete intervals of emissions values as an artifact of the population data that CDIAC's spatial distribution is based on (Figure 13e). As shown in Figure 6e, CDIAC assigns the same population density to all cells that fall within a specific state, thereby creating distinct clusters of values. At 1° resolution, Vulcan and CDIAC are poorly associated, with a spatial correlation coefficient of 0.39 (Table 3). Even at 3° resolution the correlation between Vulcan and

CDIAC is only 0.79, indicating that there is a large discrepancy between the spatial distribution and magnitude of Vulcan and CDIAC data.

At a 1° resolution the differences between two top-down approaches, FFDAS and EDGAR, nearly disappear when compared to Vulcan. If $FFCO_2$ emissions inventories are going to be used at 1° resolution then these top-down approaches estimate and distribute emissions no differently than the bottom-up approaches. If data are to be used at finer resolutions of 0.5° or 0.1°, the approach for distributing emissions begins to matter much more. However, because all of these inventories are estimates it is not possible to definitively say which approach is more accurate. Vulcan is generally considered to be the most detailed representation of emissions for the U.S. FFDAS may be considered the best global representation because it has better correlation with Vulcan for the U.S. However, Vulcan and FFDAS share the same authors, so a stronger correlation is expected between Vulcan and FFDAS. In addition, the relationships that FFDAS uses to distribute emissions may be most accurate for more developed countries like the U.S., and the quality of FFDAS's ability to distribute emissions should not be extrapolated beyond the national extent examined in this analysis.

3.1.2. Nightlights vs. Population density

Top-down $FFCO_2$ emissions inventories utilize different methods and proxy data sets for spatially disaggregating national level emissions into subnational units. ODIAC relies on nightlight data to distribute $FFCO_2$ emissions in space, while CDIAC relies on population density, for example. FFDAS utilizes both nightlight data and population in

the disaggregation of $FFCO_2$ emissions. Comparisons are made between FFDAS and ODIAC, FFDAS and CDIAC, and ODIAC and CDIAC to compare the effects of using nightlight data, population, or a combination of the two in the distribution of $FFCO_2$ emissions. The relationship between ODIAC and CDIAC is especially of interest because these data sets start with the same global and national emissions totals but use different approaches to distribute them in space. The relationship between ODIAC and FFDAS is also of interest because both datasets use nightlight data to distribute emissions.

ODIAC and CDIAC use the same emissions estimates (with in a range of 2-3%), but distribute national level emissions using different approaches. ODIAC uses nightlights data and the location of large point sources as inventoried in CARMA to distribute emissions on a 1 km grid, while CDIAC uses a 1984 population density map to distribute emissions on a 1° grid. The relationship between ODIAC and CDIAC is poor, with a correlation coefficient of 0.38 at 1° resolution and 0.76 at 3° resolution (Figure 14, Table 4).

At 0.1° resolution FFDAS and ODIAC have the best fit at cells with higher emissions magnitudes. The greatest agreement between ODIAC and FFDAS at higher emissions values reflects the tendency of both FFDAS and ODIAC to concentrate the majority of their emissions to high-emitting cells in urban areas. The distribution of ODIAC and FFDAS become much more similar at the 1° resolution, trending at the same values throughout the distribution (Figure 5). Figures 8 and 11 show that as resolution decreases the fit between FFDAS and ODIAC increases. At 0.1° resolution the correlation of

FFDAS and ODIAC is 0.92, which jumps to 0.98 at 0.5° resolution, and 0.99 at 1° resolution and lower (Figure 8, Table 4). As resolution decreases to 2° it becomes apparent that FFDAS has slightly lower values than ODIAC. When the absolute value of FFDAS and ODIAC are compared to their relative value, the emissions magnitudes cluster just below zero, reflecting the lower national total of emissions estimated by FFDAS.

As previously indicated, FFDAS and CDIAC display discrete clustering of emissions values (Figure 2 and Figure 5). However, this pattern is also seen in ODIAC. When CDIAC (Figure 14a) and FFDAS (Figure 15a) are plotted against ODIAC on a log scale, clustering of emissions values are visible in all three emissions inventories, signifying that this pattern is related to the use of nightlights and population in the distribution of emissions. This suggests that the use of nightlights data and population are not a good discriminator of emissions at lower magnitudes. However, since this pattern is present in FFDAS, ODIAC, and CDIAC, it is hard to attribute this limitation specifically to nightlight data or population. Nonetheless, the clustering seen in CDIAC only occurs because of the coarse resolution population data it is based on and the clustering in ODIAC cannot be a result of population data. Since FFDAS and ODIAC both display discrete values of emissions at low values, and both use nightlight data, this pattern may be reflective of a limitation in nightlight data rather than population.

After FFDAS and ODIAC are aggregated to 1° resolution the range of emissions values decrease and the clustering of data values become less distinct. At 3° resolution the

discrete intervals in CDIAC disappear when plotted against ODIAC (Figure 10b). At 1° resolution, the limitation in nightlight data at low values may not be significant. However the difference between FFDAS and CDIAC and ODIAC and CDIAC is poor at all resolutions, indicating that the 1° resolution population data set that CDIAC uses does not produce good agreement with other emissions inventories.

3.1.3. Treatment of Large Point Sources

While large differences between $FFCO_2$ emissions inventories may be the result using of different disaggregation methods, it is more likely that the largest difference between the data sets occurs due to the treatment of large point sources. If large point source locations are included in the distribution of $FFCO_2$ emissions, nearly half the national total of emissions has been accurately allocated in space. When high emissions values are not directly related to an urban area, they are more than likely associated with emissions from large point sources.

Emissions from the top 50 CO_2 emitting grid spaces from the eGRID database for the year 2009 are plotted against values of emissions from each $FFCO_2$ emissions inventory at the corresponding location at 0.1° (Figure 16) and 1° (Figure 17) resolutions. It should be noted that CARMA is a more commonly used LPS inventory for global FFCO2 emissions inventories than eGRID. At 0.1° resolution (Figure 16) FFDAS and ODIAC have the best agreement with emissions from large point sources, reflecting the incorporation of large point sources into these emissions inventories. At 0.1° resolution Vulcan and EDGAR have poor agreement with emissions from LPS's. This pattern is

unexpected as Vulcan places all point values in the grid cell occupied by their geocoded location. However, the Vulcan inventory uses neither eGRID nor CARMA data to estimate emissions from electrical generation, but rather relies on the EPA ETS/CEMs data, which is one input into eGRID. However, CEMs measured emissions do not always agree with emissions calculated using material balance. In addition to using different LPS data than eGRID, Vulcan is developed for the year 2002, while the eGRID data in this analysis estimates emissions for the year 2009. EDGAR reports the use of point source data in their methodology, although no reference to a specific LPS inventory is given.

At 1° resolution (Figure 17) all $FFCO_2$ emissions have values consistently equal to or higher than the large point sources located in that grid cell except for CDIAC. At the 1° resolution CDIAC has consistently lower values than other emissions inventories in cells where the top 20 large point source emitters are located (Figure 16). In the five instances where CDIAC does exceed emissions that can be attributed to large point sources, the cells are located over major cities.

3.2.Geo-referencing

Few $FFCO_2$ emissions inventories explicitly describe the geo-referencing system used to analyze and represent the data. The selection of a map projection commonly relies on the projection of the data set used to delineate the borders within which the $FFCO_2$ emissions will be distributed [*Andres et al*., 2012]. Traditionally, $FFCO_2$ emissions inventories are represented on a regular 0.1° grid using spherical coordinates. All data sets analyzed use spherical coordinates, represented in geographic coordinate system

WGS84, except for Vulcan, which was built on regular 10km grid and represented in lambert conformal conic projection and NAD83 datum. Andres et al. [2012] address the importance of map projections, recognizing that the conversion from a three-dimensional world to a two-dimensional surface can distort shape, area, distance, or direction. Mathematical equations exist to transform data from one projection to another, but the distortion caused by conversions between planar coordinate systems and three-dimensional spherical representations of the earth are important considerations that should be addressed in future analyses. Map projections are especially important when $FFCO_2$ emissions inventories are going to be used in a model with a specific, and possibly different, map projection built into it [*Andres et al*., 2012].

3.3.Scale Issues

The power of a geographic information system (GIS) lies in its ability to transform, analyze and manipulate geographic data, however, all of these abilities rely on measurements of scale [*Goodchild,* 2011]. The primary questions considered in geographic studies are what the appropriate extent and resolution is to examine a specific geographic phenomenon [*Cao and Lam,* 1997]. In geography, the concept of ecological fallacy describes the practice of attributing characteristic of data from a large scale to smaller scales [*Cao and Lam*, 1997; *Goodchild*, 2001, 2011]. Global $FFCO_2$ emissions totals are not used to characterize national level $FFCO_2$ emissions totals since total CO_2 emissions at the national scale do not agree with total emissions at the global scale. Therefore, attributing national level emissions to subnational scales may represent a form of ecological fallacy, in which data at a larger scale is erroneously attributed to a smaller

scale. In addition, while there are proxies used in the disaggregation of $FFCO_2$ emissions inventories, the relationships between proxies are scale dependent. For example, population density is not a good proxy for $FFCO_2$ at fine scales [*Andres et al.,* 2011]. If top-down approaches incorporate errors of ecological fallacy and spatial dependence, bottom-up approaches may be a stronger approach for estimating subnational $FFCO_2$ emissions. However, data are often only available at scales that are too coarse for modeling a given process at the correct scale. Models that predict the effects of scale on the properties of data without actually acquiring data at those scale are useful for evaluating the impacts of using data that are too coarse for their purpose [*Goodchild,* 2001]. However, because the Vulcan inventory was acquired at such fine scales it is possible to measure the impacts of using data that are too coarse for their purpose. Models are also capable of simulating the disaggregation of data so that there is good agreement between the simulated data and the expected data. While some of the proxies used to disaggregate emissions are scale dependent, future simulations may address more accurate and complex methods for disaggregation.

When masking global $FFCO_2$ emissions inventories to the Vulcan extent, national level emissions from one inventory may not be captured if that emissions inventory uses a different boundary definition for the continental U.S., making comparisons of U.S. national totals across $FFCO_2$ emissions inventories using this methodology imprecise. One example of differing boundaries is shown in Figure 6e and 7e, where CDIAC contains zero-magnitude cells along the border where other emissions inventories assign non-zero values. In general, the effects of border issues can be seen in lower emissions

values along the outward edge of all emissions inventories at 0.5°, 1° (Figure 6), and 2° (Figure 7) resolutions. There are also higher standard deviations along boundaries in this analysis, indicating poor agreement along the edges of clipped data (Figure 18e and 18f).

Additionally, when masking data at the global scale to a national extent, issues arise as to whether or not it is more appropriate to first aggregate the data at the global scale, and then mask it to the national scale, or to first mask the data and then aggregate. If the data is first aggregated and then masked to the extent of Vulcan, the coarser resolutions capture a higher magnitude of emissions from outside the U.S., causing emissions at the national level to increase with resolution. Aggregating the global data sets after they have been masked produces consistent national totals but misleadingly excludes data values that may be relevant, depending on the national boundary definition for that data set. In particular, smaller magnitudes and higher standard deviations are seen in cells along the Canada and Mexico borders, where emissions at the global scale were clipped to the national extent of Vulcan.

Across each comparison made in this study, aggregating the $FFCO_2$ emissions inventories to coarser resolutions produced better correlation between the datasets. However, while the correlations increased, previous studies in geography indicate that the improvements correlation at aggregated resolutions tend to be offset by the loss of degrees of freedom, making the relationships between aggregated data no more significant [*Goodchild*, 2011].

3.4.Uncertainty across emissions inventories

While comparing $FFCO_2$ emissions inventories against the distributions, magnitudes, and inputs of other $FFCO_2$ emissions inventories lends great insight into the effects of methods and data on $FFCO_2$ emissions estimates, it does not fully capture the uncertainty that arises from the variability of $FFCO_2$ emissions estimates.

In a first attempt to estimate uncertainty across $FFCO_2$ emissions inventories, maps of the average emissions for the U.S. for the year 2002 were generated at 0.1° and 1° resolution (Figures 18a and 18b). Averages for the year 2002 include emissions from EDGAR, FFDAS, and Vulcan at 0.1° resolution and EDGAR, FFDAS, Vulcan, and CDIAC at 1° resolution. The standard deviation across datasets was also mapped for the year 2002 at 0.1° and 1° resolution (Figure 18c and 18d). The standard deviation was divided by the mean to produce a map of the coefficient of variation, which compares the relative magnitude to the variance at each grid cell (Figure 18e and 18f).

The spatial distribution of emissions is not significantly different at 0.1° or 1° resolutions. Emissions magnitudes have the highest standard deviations where the most emissions are located, i.e. in major urban areas (Figure 18c and 18d). Areas which have the highest emissions are the most important locations for emissions inventories to agree on, as these areas have greater impact on fossil fuel carbon dioxide emissions and have greater policy implications for the monitoring and reduction of carbon dioxide emissions. However, after the standard deviation is normalized to the emissions magnitude, and the coefficient

of variance is calculated, the greatest relative disagreement between emissions inventories occurs at lower emissions values.

4. Conclusions

Each of the approaches compared in this paper is known to have both strengths and weaknesses. Bottom-up approaches are more detailed, but are also more time and labor intensive. Top-down approaches are less time intensive, but are not as detailed and rely on fuzzy relationships that change with scale [*Rayner* et al., 2010]. For example, disaggregation by nightlights relies on a relationship between nightlight data and population, and correlations between population and CO_2 emissions that are not exact [*Rayner* et al., 2010; *Oda and Maksyutov,* 2011].

At coarser resolutions (1° and higher) distinctive differences in the patterns are hard to detect, but at finer resolutions distinct patterns and relationships between datasets become apparent as functions of inputs and methods used in their creation. The results presented in this analysis reveal that primary differences between data sets are related to differences in top-down and bottom-up approaches, the use of night lights versus population density in the spatial distribution of emissions, and the treatment of large point sources in the emissions inventory. The best fit between $FFCO_2$ emissions inventories occurs between FFDAS and ODIAC, both of which rely heavily on nightlights data. CDIAC shows the least correlation to any of the $FFCO_2$ emissions inventories. As a function of CDIAC's coarse resolution it is unable to fully capture the fine distribution of emissions that occurs sub-nationally. Additionally, the lack of consideration for emissions from large point

sources in CDIAC increases differences in the spatial distribution of $FFCO_2$ in CDIAC and the other four $FFCO_2$ emissions inventories. Therefore, the distinction between point source data and non-point source data in the creation of spatially explicit $FFCO_2$ emissions inventories is critical.

The unique patterns presented in EDGAR should be further analyzed after more detailed information on the methodologies can be obtained or are published. In order for these $FFCO_2$ emission inventories to be used to their fullest potential more detailed methodologies should be published and maintained for each data set. Vulcan has the most comprehensive documentation, allowing for a better understanding of how the inputs and method of spatial allocation influence the spatial distribution of emissions in Vulcan compared to other inventories. Future research should also investigate the strengths and weaknesses of nightlight data in distribution emissions related to specific activities. For example, nightlights data may be more strongly related to residential or commercial emissions versus transportation and industrial sources of emissions. An expanded analysis into the differences in urban emissions profiles for major U.S. cities could also lend insight into what is happening in these very important sources of $FFCO_2$ emissions.

The differences among these five spatial $FFCO_2$ emissions inventories are visible both graphically and numerically, but are far from encapsulating the uncertainty associated with current methodologies for representing $FFCO_2$ emissions in space. While there is better correlation between the data sets at coarser resolutions, there is also a considerable amount of information loss. The comparison of these five $FFCO_2$ emissions inventories

across multiple resolutions brings into question whether or not coarser resolution emissions inventories are more accurate because they have better agreement with each other, or if the loss of information makes the use of aggregated data more uncertain.

While atmospheric concentrations of carbon and carbon from fossil fuel combustion are considered the least uncertain values in the global carbon cycle, there is still a lot of uncertainty associated with our understanding of $FFCO_2$ emissions inventories. Uncertainties in the global carbon cycle limit our ability to effectively measure, monitor, or verify where, when, and how much carbon is being emitted from fossil fuel sources. However, by developing a cohesive carbon monitoring system that seeks to develop best practice methodologies for quantifying carbon, uncertainties in the carbon cycle can eventually be reduced. In addition, such a carbon monitoring system will allow for the monitoring and verification of international agreements, which seek to limit carbon emissions globally. Ultimately, the decision to use top-down versus bottom-up approaches depends on what the data are going to be used for, which will ultimately determine if the collection of data at finer resolution is worth the cost.

Acknowledgements

The data for this paper is available at the following locations:

CDIAC 1° X 1° gridded FFCO2 emissions distribution can be found at http://cdiac.ornl.gov .

EDGAR 0.1° X 0.1° gridded FFCO2 emissions distribution can be found at http://edgar.jrc.ec.europa.eu .

FFDAS 0.1° X 0.1° gridded FFCO2 emissions distribution can be requested at http://gurney.faculty.asu.edu/research/ffdas.php .

ODIAC 0.1° X 0.1° gridded FFCO2 emissions distribution can be requested at http://odiac.org .

eGRID electrical generating unit LPS data can be found at http://www.epa.gov/cleanenergy/energy-resources/egrid/index.html .

CARMA LPS power plant data can be found at http://carma.org/ .

Energy statistics data from each agency can be found at the following sources:

IEA statistics can be found at http://www.iea.org/statistics/ .

DOE/EIA statistics can be found at: http://www.eia.gov/ .

U.N. statistics can be found at: http://unstats.un.org/unsd/energy/ .

BP statistics can be found at http://www.bp.com/en/global/corporate/about-bp/energy-economics.html .

Funding for this research comes from the Carbon Monitoring System Program (NNH11ZDA001N-CMS) of the U.S. National Aeronautics and Space Administration.

References

Andres, R.J., T.A. Boden, F. –M, Breon, P.Ciais, S. Davis, D. Erickson, J.S. Gregg, A. Jacobson, G. Marland, J. Miller, J., T. Oda, J.G. Olivier, M.R. Raupach, P. Rayner, and K. Treanton (2012), A synthesis of carbon dioxide emissions, Biogeosceiences Discussions, 9, 1299-1376, doi:10.5194/bgd-9-1299-2012.

Andres, R.J, J.S. Gregg, L. Losey, G. Marland, and T.A. Boden (2011), Monthly, global emissions of carbon dioxide from fossil fuel consumption, Tellus B, 63(3), 309-327, doi:10.1111/j.1600-0889.2011.00530.x.

Blasing, T.K., G. Marland, and C. Broniak. Estimates of annual fossil-Fuel CO_2 emitted for each state in the U.S.A and the District of Columbia for each year from 1960 through 2001, Carbon Dioxide Information Analysis Center, Oak Ridge National Laboratory, U.S. Department of Energy, Oak Ridge, TN, U.S.A. doi 10.3334/CDIAC/00003.

Cao, C. and Nina Siu-Ngan Lam (1997), Understanding the scale and resolution effects in remote sensing, in Scale in Remote Sensing and GIS, edited by Dale A. Quattrochi and Michael F. Goodchild, pp. 57 – 72, Boca Raton, Florida, CRC/Lewis Publishers.

Dai, J., and D. M. Rocke (1999), A GIS-based approach to spatial allocation of area source solvent emissions, Environmental Modelling and Software, 15(3), 293-302, doi:10.1016/S1364-8152(00)00004-9.

Goodchild, M. F. (2001), Models of scale and scales of modelling, in Modelling Scale in Geographical Information Science, edited by Nicholas J. Tate and Peter M. Atkinson, pp. 3 - 10, West Sussex, England, John Wiley & Sons, Ltd.

Goodchild, M. F. (2011), Scale in GIS: An overview, Scale Issues in Geomorphology, 130(1-2), 5-9, doi: 10.1016/j.geomorph.2010.10.004.

Gregg, J.S., and R.J. Andres (2008), A method for estimating the temporal and spatial patterns of carbon dioxide emissions from national fossil-fuel consumption, Tellus, 60(1), 1-10, doi:101.1111/j.1600-0889.2007.00319.x.

Gurney, K.R., D.L. Zhour, Y. Mendoza, C. Miller, S. Geethakumar, and S. de La Rue du can (2009), High resolution fossil fuel combustion CO_2 emission fluxes for the United States, Environmental Science and Technology, 43(14), 5535-5541, doi:10.1021/es900806c.

Hartmann, D.L., A.M.G. Klein Tank, M. Rusticucci, L.V. Alexander, S. Brönnimann, Y. Charabi, F.J. Dentener, E.J. Dlugokencky, D.R. Easterling, A. Kaplan, B.J. Soden, P.W. Thorne, M. Wild, and P.M. Zhai (2013), Observations: atmosphere and surface, in Climate Change 2013: The Physical Science Basis. Contribution of Working Group I to the Fifth Assessment Report of the Intergovernmental Panel on Climate Change, edited by T.F. Stocker, D. Qin, G.K. Plattner, M. Tignor, S.K. Allen, J. Boschung, A. Nauels, Y. Xia, V.

Bex and P.M. Midgley, pp. 159-255, Cambridge University Press, Cambridge, United Kingdom and New York, NY, USA.

Marland, G., A. Brenkert, and J. Olivier (1999), CO_2 from fossil fuel burning: a comparison of ORNL and EDGAR estimates of national emissions, Environmental Science and Policy, 2(3), 265-273, doi:10.1016/S1462-9011(99)00018-0.

Oda, T., and S. Maksyutov (2011), A very high-resoltuion (1 km X 1 km) global fossil fuel CO_2 emission inventory derived using point source database and satellite observations of nighttime lights, Atmospheric Chemistry and Physics, 11, 543-556, doi:10.5194/acp-11-543-2011.

Rayner, P.J., M.R. Raupach, M. Paget, P. Peylin, and E. Koffi (2010), A new global gridded data set of CO_2 emissions from fossil fuel combustion: Methodology and evaluation, Journal of Geophysical Research, 115 (D19306), doi:10.1029/2099JD013439.

Singer, A., M. Branham, M.G. Hutchins, J. Welker, D. Woodard, C. Badurek, T. Ruseva, E. Marland, and G. Marland (2014), The Role of CO_2 emissions from Large Point Sources in Emissions Totals, Responsibility, and Policy, Environmental Science and Policy, in press.

Table 1: An overview of $FFCO_2$ emissions inventories analyzed

	CDIAC	EDGAR	FFDAS	ODIAC	Vulcan
Years Analyzed	2002, 2008	2002, 2008	2002, 2008	2008	2002
Approach	Top- down	Top- down	Model-data fusion	Top- down	Bottom- up
Version	V4.2 FT2010	V2013	6/28/2014	2/6/2014	V2.2
Energy Stats.	IEA, U.N., Commercial	U.N.	IEA	CDIAC	EPA, NMIM, Aero2k
Scale and Resolution	Global, 1°	Global, 0.1 °	Global, 0.1 °	Global, 1 km	U.S., 0.1 °
Websites	http://edgar.jrc.ec.europa.eu	http://cdiac.ornl.gov/	http://gurney.faculty.asu.edu/research/ffdas.php	http://odiac.org/dataset.html	http://vulcan.project.asu.edu/research.php
Large Point Sources	Included	N/A	N/A	CARMA	NEI and ETS/CEMS
Sectors	Energy, Industrial processes, Solvent and other product use	Fossil fuel combustion, Cement manufacture, Gas flaring in oil fields	Energy, Manufacturing, Industrial, Transport, Other (residential, agriculture, fishing)	Fossil fuel combustion, Cement manufacture, Gas flaring in oil fields	Air, Cement, Commercial, Residential, Industrial, Cement manufacture, Utilities, On-road and Non-road
Spatial Distribution	Location of LPS, road network, shipping & aviation routes, population density	Population	Nightlights, Population, GDP, Energy intensity, Carbon intensity	Nightlights and location of large point sources	Road networks, location of large point sources, total sq. floor footage of buildings

Table 2: Author-documented totals compared to user calculated global and national totals

Data	Author-Documented Total (Tonnes C)	Global Calculated Total (Tonnes C)	U.S. Calculated Total (Tonnes C)
Vulcan	2002: 1,541,353,052.7 (U.S.)	N/A	1,541,353,000
ODIAC	2008: 8,468,120,000 (±2-3%)	8,468,069,000	1,533,826,000
FFDAS	2002: 6,222,573,500 2008: 7,617,185,500	2002: 6,222,573,000 2008: 7,617,185,000	2002: 1,396,513,000 2008: 1,380,671,000
CDIAC	2002: 6,712,000,000 2008: 8,288,000,000	2002: 6,711,645,000 2008: 8,287,658,000	2002: 1,505,423,000 2008: 1,509,024,000
EDGAR	?	2002: 7,041,831,063 2008: 8,654,032,698	2002: 1,519,385,000 2008: 1,499,356,000

Table 3: Correlation Coefficients and Sum of Absolute Differences (SAD)in MtC (megatonne of Carbon) for the year 2002

	FFDAS vs. Vulcan		**EDGAR vs. Vulcan**		**FFDAS vs. EDGAR 2002**		**EDGAR vs. CDIAC 2002**		**Vulcan vs. CDIAC 2002**	
	Corr.	SAD	Corr.	SAD	Corr.	SAD	Corr.	SAD	Corr.	SAD
0.1	0.62	1172	0.43	1494	0.37	1404	-	-	-	-
0.5	0.91	521	0.55	663	0.89	650	-	-	-	-
1	0.95	392	0.94	468	0.94	469	0.35	1603	0.39	1650
2	0.97	292	0.97	311	0.97	320	0.71	1012	0.72	1034
3	0.98	248	0.98	271	0.98	262	0.77	839	0.79	805

Table 4: Correlation Coefficients and Sum of Absolute Differences (SAD)in MtC (megatonne of Carbon) for the year 2008

	FFDAS vs. ODIAC		**EDGAR vs. ODIAC 2008**		**FFDAS vs. EDGAR 2008**		**EDGAR vs. CDIAC 2008**		**ODIAC vs. CDIAC 2008**	
	Corr.	SAD	Corr.	SAD	Corr.	SAD	Corr.	SAD	Corr.	SAD
0.1	0.92	500	0.39	1419	0.37	1390	-	-	-	-
0.5	0.98	259	0.89	661	0.88	637	-	-	-	-
1	0.99	214	0.94	468	0.93	470	0.35	1603	0.38	1662
2	0.99	174	0.97	319	0.96	326	0.71	1007	0.70	1037
3	1.00	164	0.98	246	0.98	264	0.78	832	0.76	898

Figure Captions

Figure 1: Cumulative emissions curves for Vulcan (2002), ODIAC (2008), FFDAS (2002 & 2008), and EDGAR (2002 & 2008) at 0.1-degree resolution. Values are compared at 81,841 non-zero grid cells in the 0.1-degree resolution Vulcan dataset. Solid lines represent data for 2002, while dashed line represent data for 2008.

Figure 2: Distributed emissions for Vulcan (2002), ODIAC (2008), FFDAS (2002 & 2008), and EDGAR (2002 & 2008) at 0.1-degree resolution. Emissions are arranged in ascending order of emissions and plotted against their point ID. Data are displayed on a log scale to highlight both high and low values.

Figure 3: Spatial distribution of the most recent years of Vulcan (a), ODIAC (b), EDGAR (c), and FFDAS (d) at 0.1-degree resolution. Data are represented on a log scale in order to display the data from different inventories on the same color ramp, and to highlight both high and low emissions values. As a result of representing the data on a log scale, values of zero do not appear on the color ramp. Zero values are instead represented by the color black.

Figure 4: Cumulative emissions curves for Vulcan (2002), ODIAC (2008), FFDAS (2002 & 2008), EDGAR (2002 & 2008), and CDIAC (2002 & 2008) at 1-degree resolution. There are 928 non- zero grid cells in the 1-degree resolution Vulcan dataset. Solid lines represent data for 2002, while dashed line represent data for 2008.

Figure 5: Distributed emissions for Vulcan (2002), ODIAC (2008), FFDAS (2002 & 2008), EDGAR (2002 & 2008), and CDIAC (2002 & 2008) at 1-degree resolution. Emissions are arranged in ascending order of emissions and plotted against their point ID. Data are displayed on a log scale to highlight both high and low values.

Figure 6: Spatial distribution of the most recent years of Vulcan (a), ODIAC (b), EDGAR (c), FFDAS (d), and CDIAC (e) at 1-degree resolution. Data are represented on a log scale in order to display the data from different inventories on the same color ramp, and to highlight both high and low emissions values. As a result of representing the data on a log scale, values of zero do not appear on the color ramp. Zero values are instead represented by the color black.

Figure 7: Spatial distribution of the most recent years of Vulcan (a), ODIAC (b), EDGAR (c), FFDAS (d), and CDIAC (e) at 2-degree resolution. Data are represented on a log scale in order to display the data from different inventories on the same color ramp, and to highlight both high and low emissions values. As a result of representing the data on a log scale, values of zero do not appear on the color ramp. Zero values are instead represented by the color black.

Figure 8: Correlation coefficients are plotted against resolution to depict the correlation threshold at the resolution at which emissions inventories show the most agreement. FFDAS is represented in yellow, EDGAR is represented in gray, and CDIAC is represented in orange. Solid line represent the above inventories (FFDAS, EDGAR, and CDIAC) compared to Vulcan (2002), while dashed lines represent each inventory compared to ODIAC (2008).

Figure 9: Difference maps for the least (a) and most (b) correlated emissions inventories at 0.1-degree resolution. Note the color ramps are not on the same scale.

Figure 10: Difference maps for the least (a, c) and most (b, d) correlated emissions inventories at 1-degree resolution for 2002(a, b) and 2008(c, d). Note the color ramps are not on the same scale.

Figure 11: Transect profile of $FFCO_2$ emissions across three U.S. cities: Baltimore, Philadelphia, and New York. FFDAS is represented in yellow, EDGAR is represent in gray, and ODIAC is represented in green.

Figure 12: The 'three-prong' distribution of EDGAR, representing the tendency of EDGAR to either agree with another emissions inventory or to significantly over- or under- estimate it.

Figure 13: Vulcan (bottom-up approach) compared to three top-down emissions inventories. Vulcan is compared to EDGAR and FFDAS at 0.1-degree resolution (a, b) and to EDGAR, FFDAS, and CDIAC at 1-degree resolution (c, d, e).

Figure 14: Log of ODIAC versus the log of CDIAC at 1- and 3-degree resolutions. ODIAC and CDIAC use the same global and national totals but distribute emissions at the sub-national scale using different spatial proxies.

Figure 15: Log of FFDAS versus the log of ODIAC at 0.1-, 0.5-, 1- and 2-degree resolutions. ODIAC and FFDAS use different global and national emissions totals, but both use nightlight data as a spatial proxy to distribute emissions sub-nationally. FFDAS also uses population as a spatial proxy, while ODIAC does not.

Figure 16: The emissions values of EDGAR, FFDAS, ODIAC, and Vulcan corresponding to the top 50 electricity-generating LPS emitting grid cells from eGRID. Point sources from eGRID (2009) were converted to a 0.1-degree grid and the top 50 emitting cells were compared to emissions values of each FFCO2 emissions inventory at 0.1-degree resolution.

Figure 17: The emissions values of CDIAC, EDGAR, FFDAS, ODIAC, and Vulcan corresponding to the top 50 electricity-generating LPS emitting grid cells from eGRID. Point sources from eGRID (2009) were converted to a 1-degree grid and the top 50 emitting cells were compared to emissions values of each FFCO2 emissions inventory at 1-degree resolution.

Figure 18: The average, standard deviation, and normalized standard deviation (coefficient of variance) were calculated for the year 2002 at 0.1-degree (a, c, and e) and 1-degree resolutions (b, d, and f).Note that the color ramps are on different scales and are not equal in magnitude across maps. Because the range of values varies between maps, leaving the color ramps on different scales better highlights the differences in the spatial distribution rather than magnitude of differences.

Figures

Figure 1: Cumulative Emissions, 0.1 degree resolution

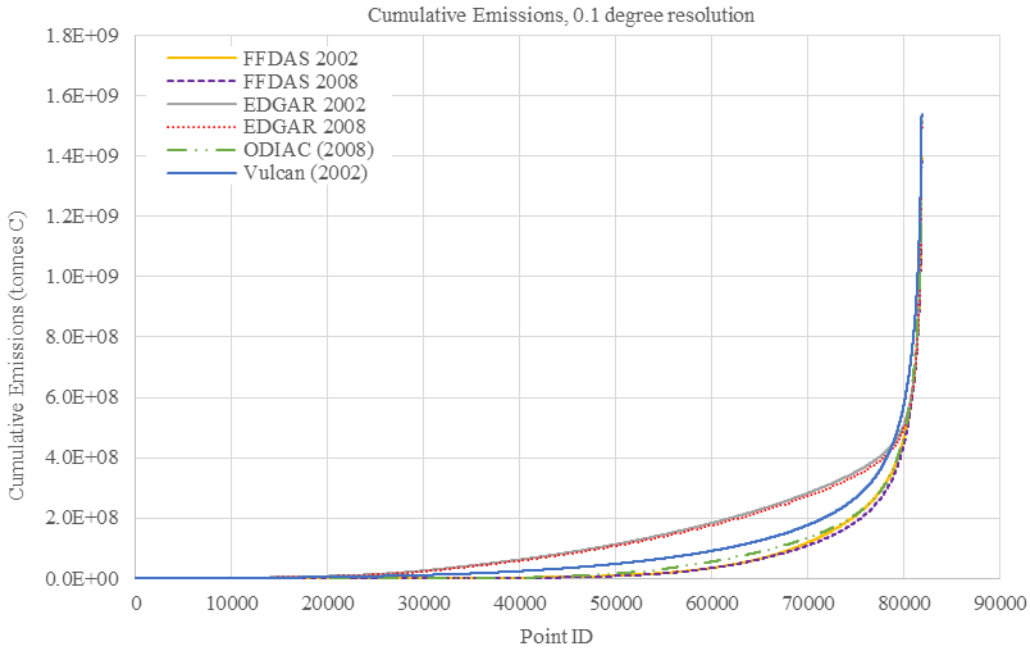

Figure 2: Distribution of Emissions, 0.1 degree resolution

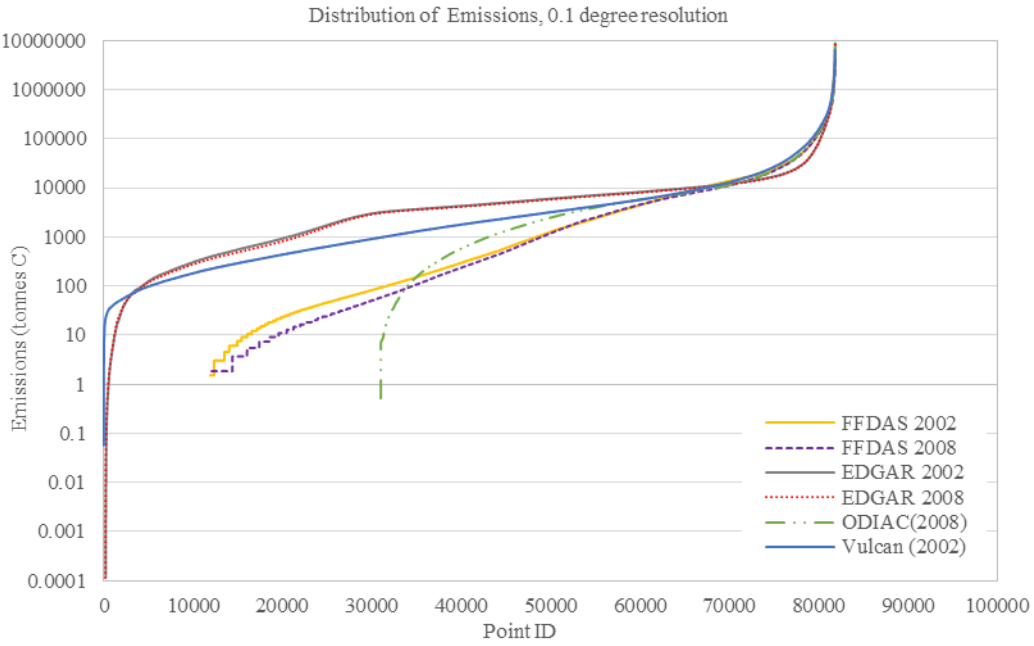

Figure 3: Spatial Distribution of FFCO2 Emissions Inventories, 0.1 degree resolution

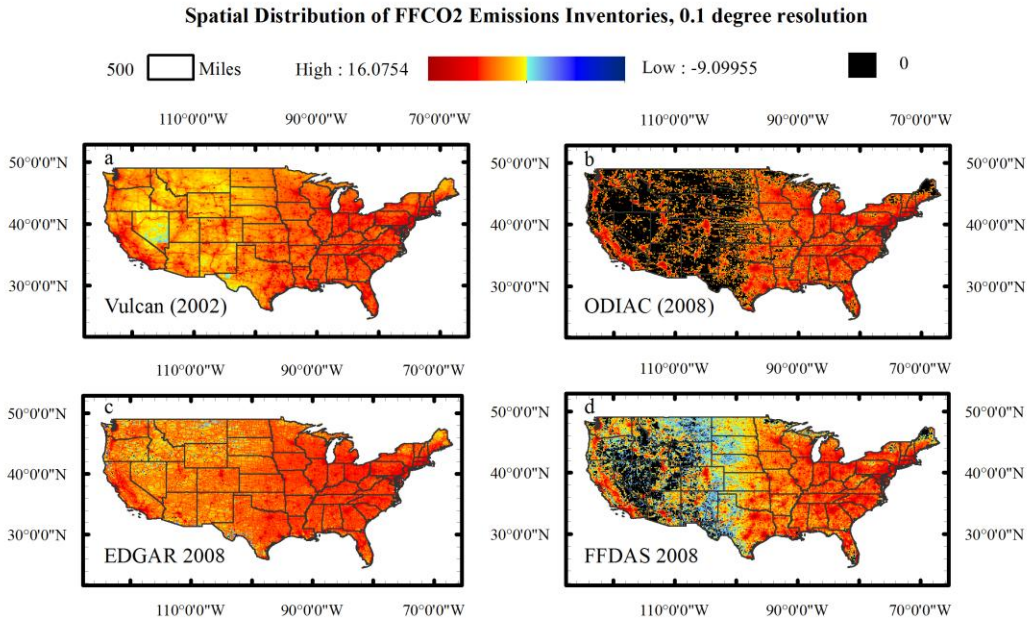

Figure 4: Cumulative Emissions, 1 degree resolution

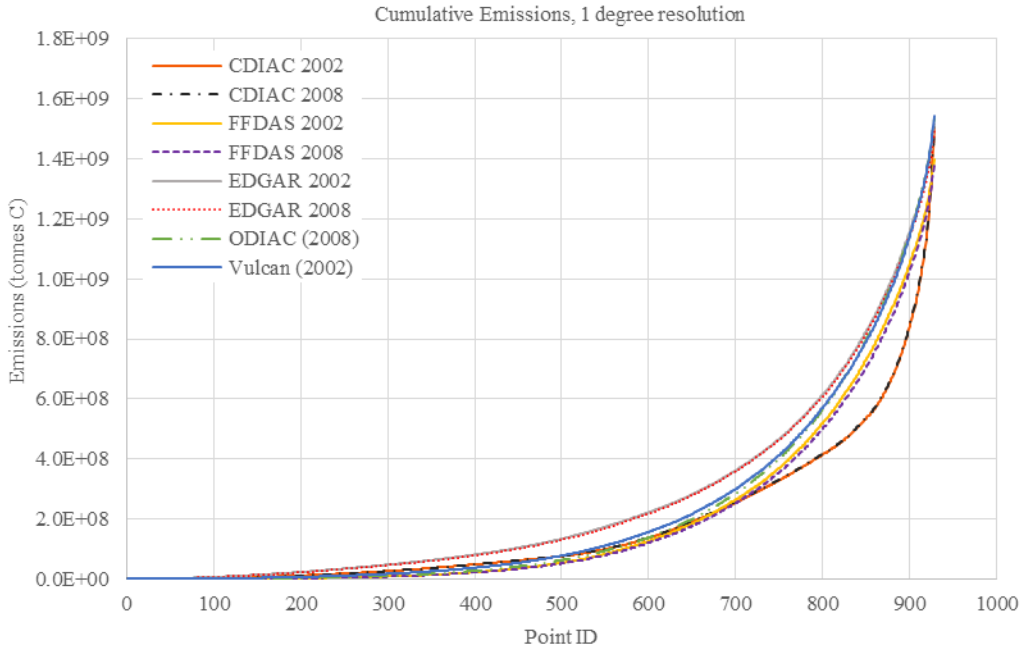

Figure 5: Distribution of Emissions, 1 degree resolution

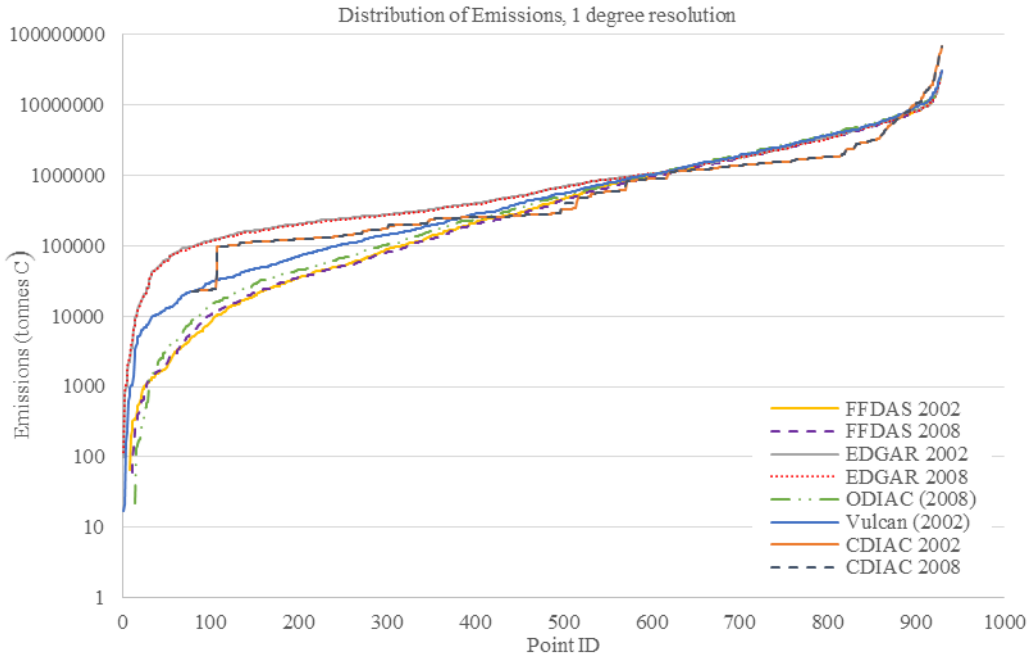

Figure 6: Spatial Distribution of FFCO2 Emissions Inventories, 1 degree resolution

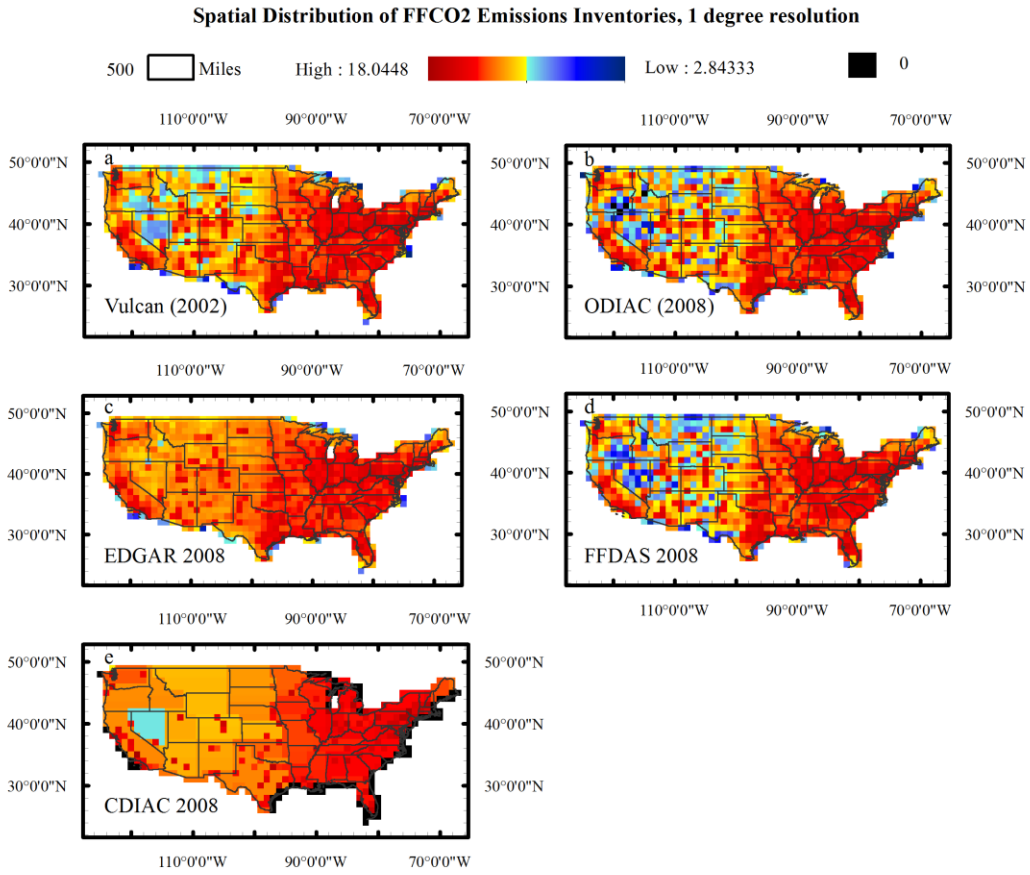

Figure 7: Spatial Distribution of FFCO2 Emissions Inventories, 2 degree resolution

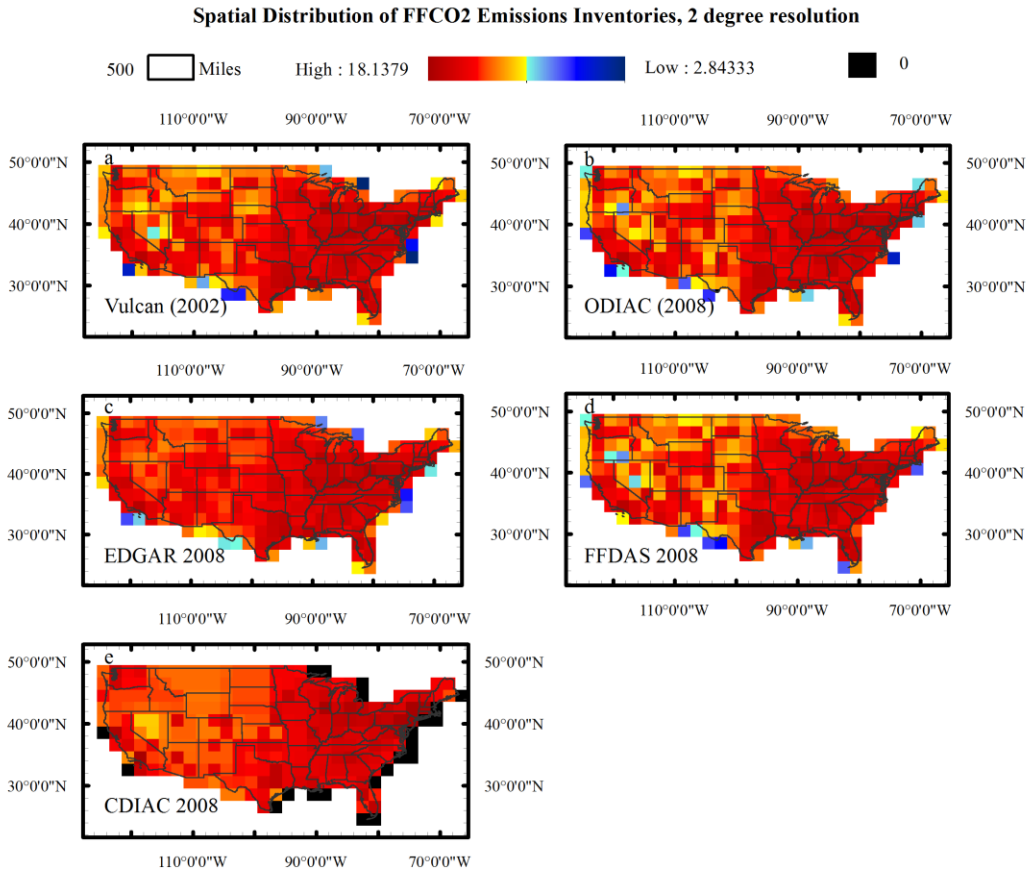

Figure 8: Correlation Thresholds

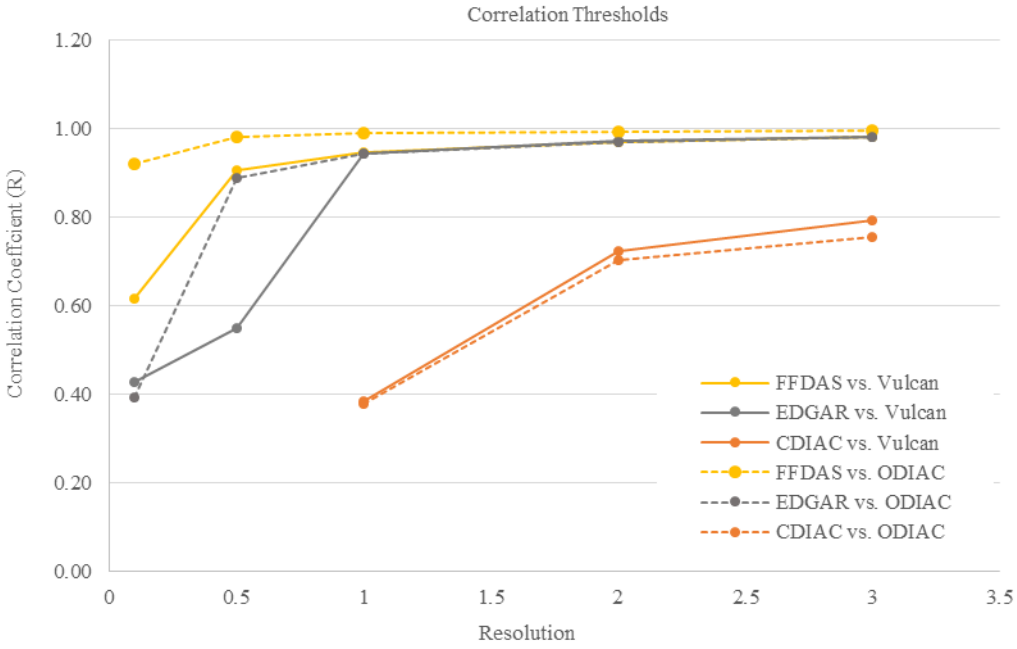

Figure 9: Differences between Emissions Inventories, 0.1 degree resolution

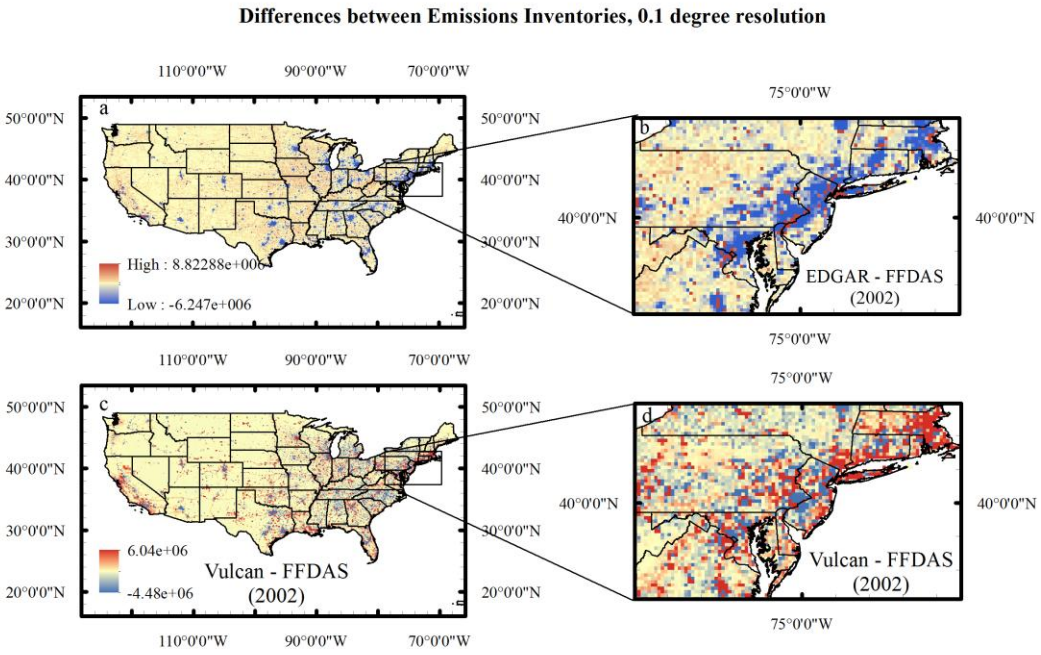

Figure 10: Differences between Emissions Inventories, 1 degree resolution

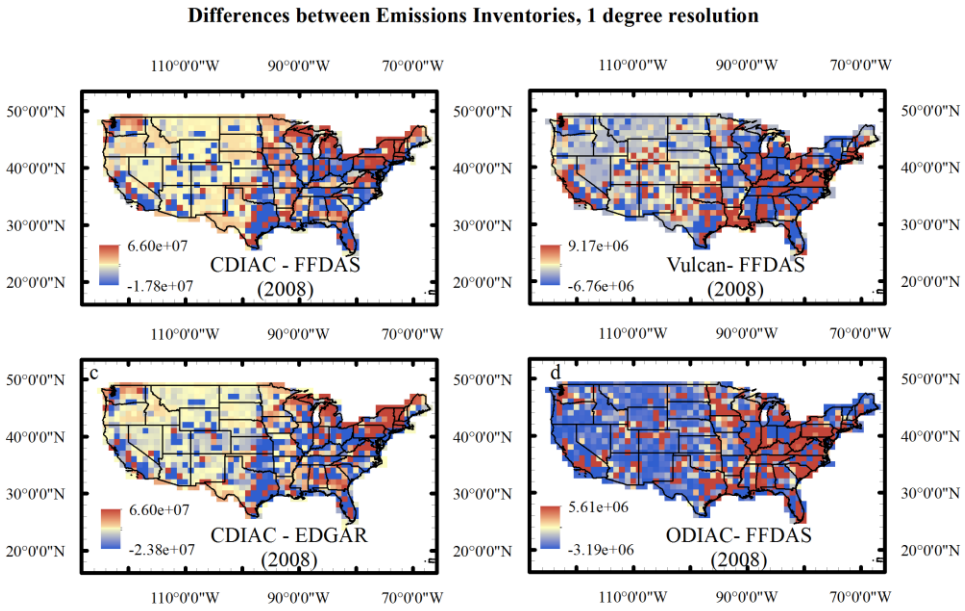

Figure 11: Emissions Profile of FFDAS, EDGAR, and ODIAC through 3 U.S. Cities, 0.1 degree resolution

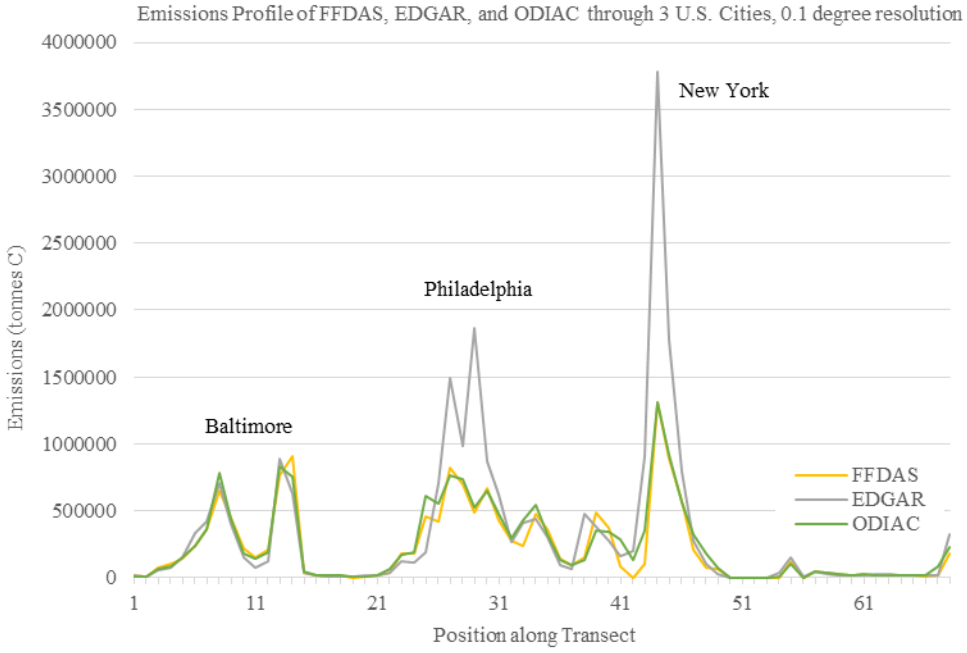

Figure 12: EDGAR versus FFDAS and ODIAC, 2008

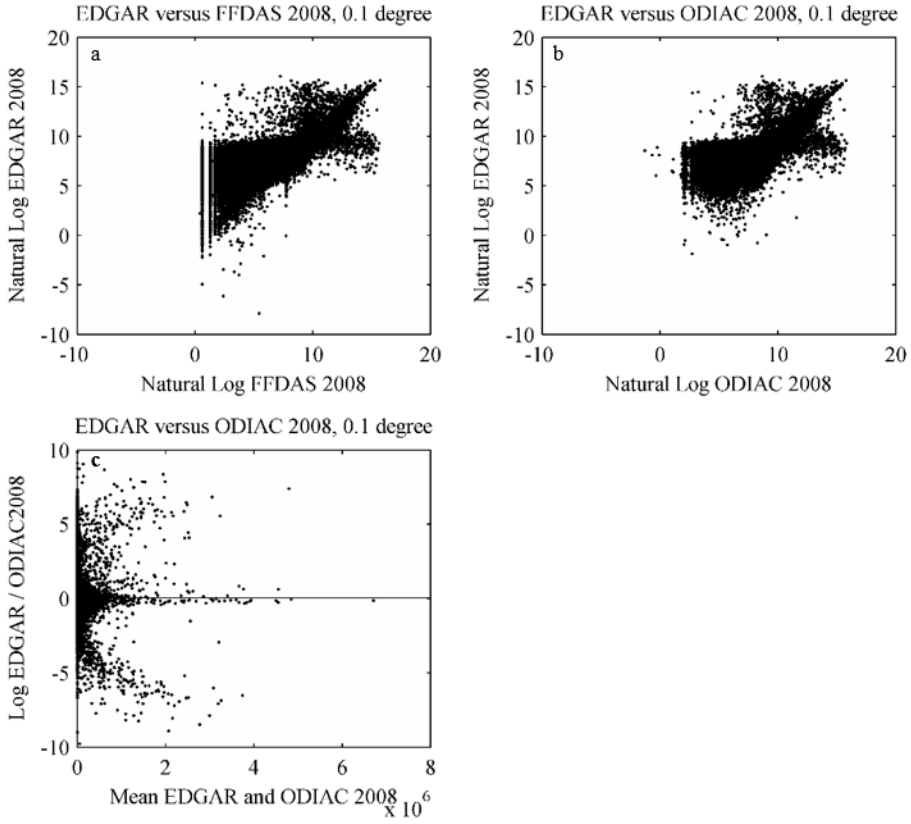

Figure 13: Vulcan versus FFDAS, EDGAR, and CDIAC, 2002

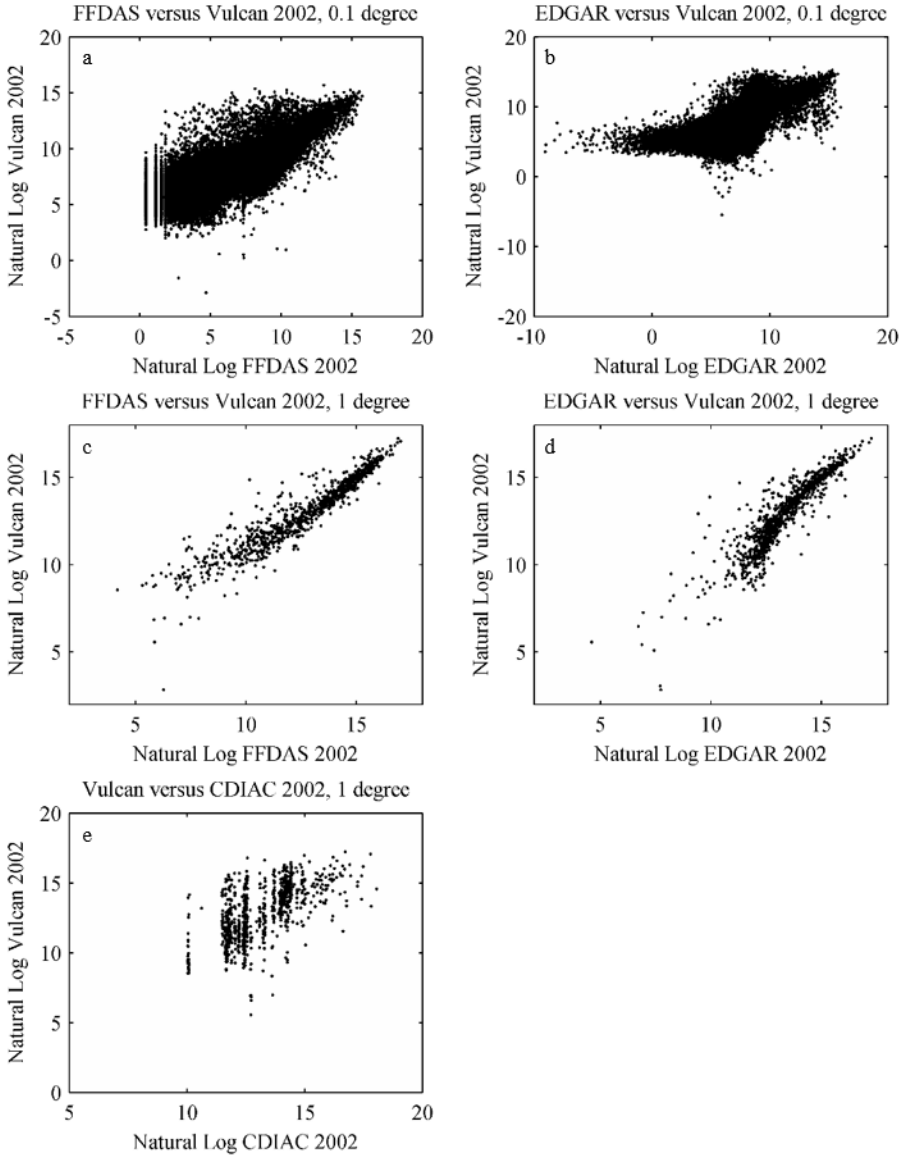

Figure 14: CDIAC versus ODIAC, 2008

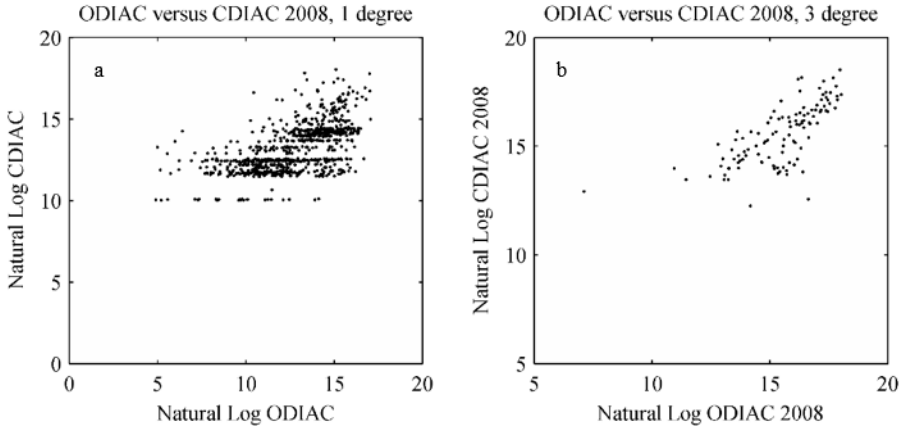

Figure 15: FFDAS versus ODIAC, 2008

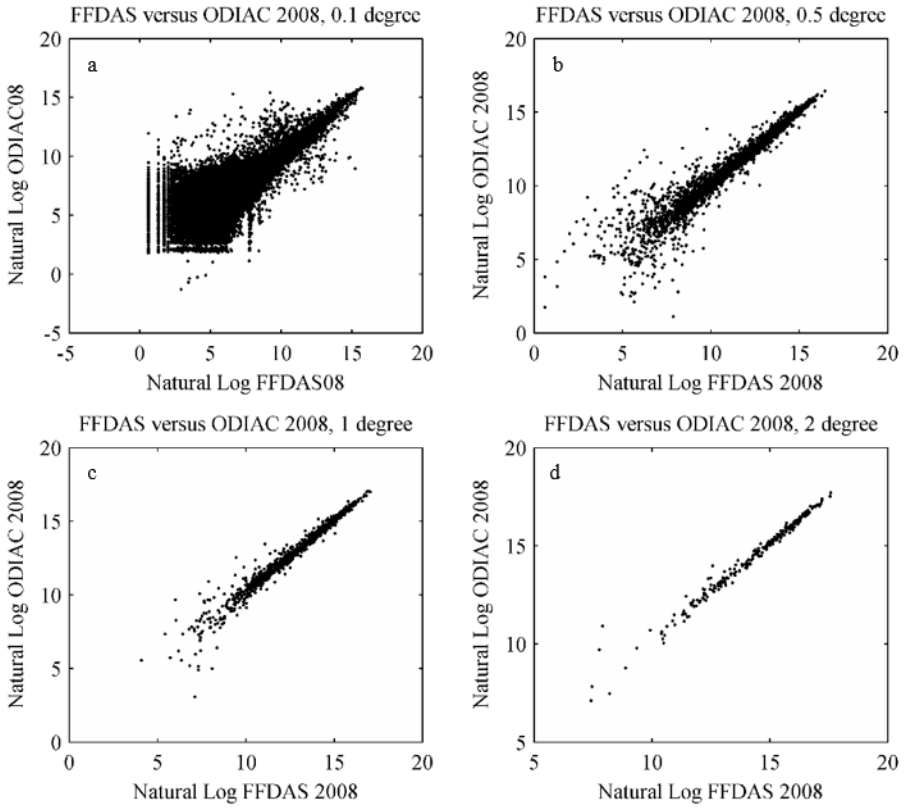

Figure 16: Top 50 LPS grid cells, 0.1 degree resolution

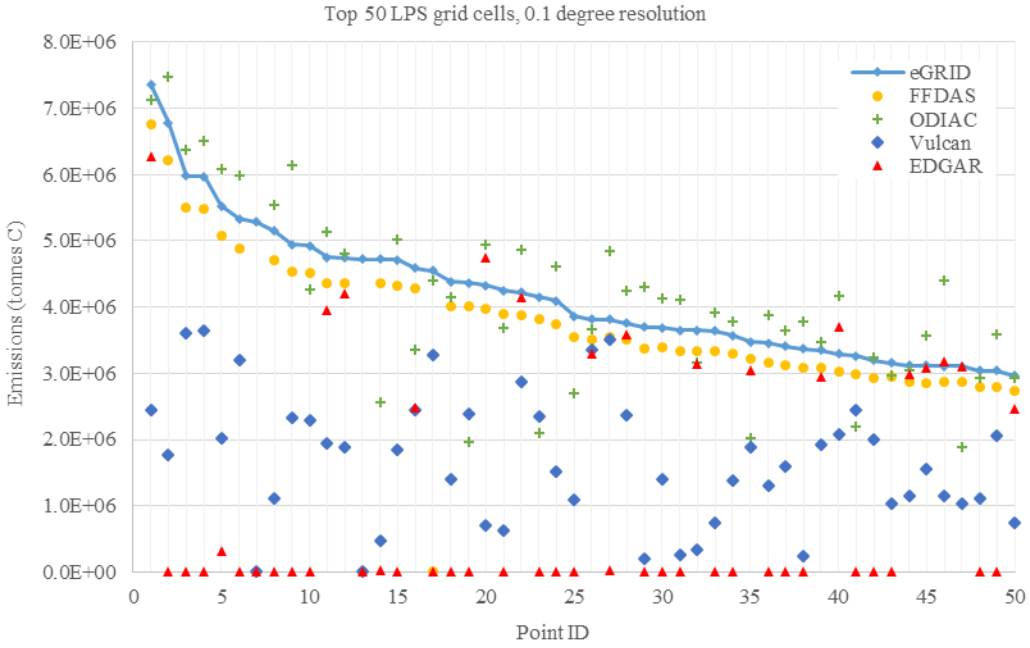

Figure 17: Top 50 LPS grid cells, 1 degree resolution

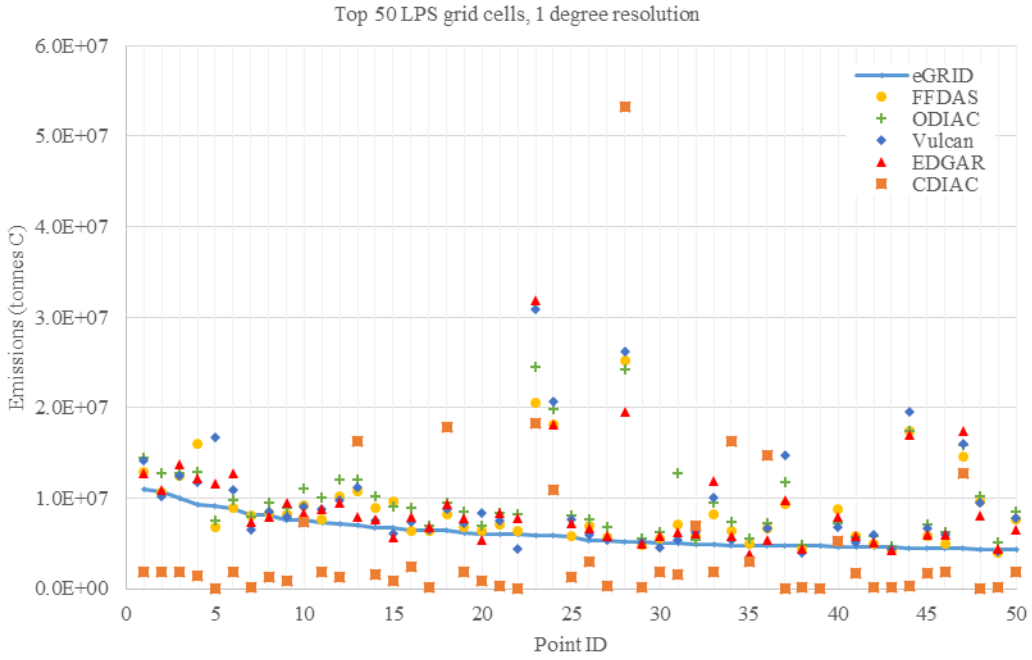

Figure 18: Mean and Variance of Emissions Inventories for 2002

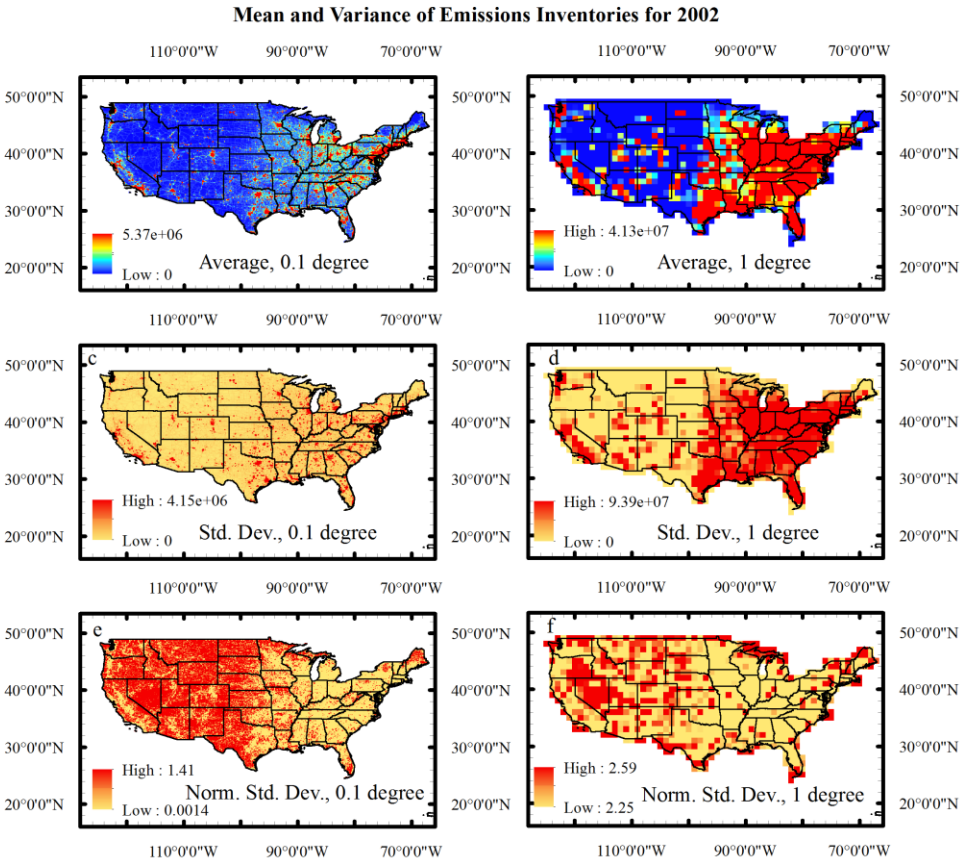

Vita

Maya Gabrielle Hutchins was born in Boone, NC to Connie and Bill Hutchins. She graduated from Watauga High in 2008. The following autumn she entered Appalachian State University and graduated in May 2012 with a B.S. in Environmental Science. In the fall of 2012 she accepted a research assistantship in Geography at Appalachian State University and began study toward a Master of Arts degree. The M.A. was awarded August 2014. In August 2014, Maya commenced work toward her Ph.D. in Geography at Arizona State University.